Engineering Structures 179 (2019) 367–386

Contents lists available at ScienceDirect

Engineering Structures

journal homepage: www.elsevier.com/locate/engstruct

Design of shear pocket connection in full-depth precast concrete deck systems

Raed Tawadrous[a,*], George Morcous[b]

[a] EConstruct, Florida, 3452 Lake Lynda Drive Suite 350, Orlando, FL 32817, USA

[b] Durham School of Architectural Engineering and Construction, College of Engineering, University of Nebraska–Lincoln, 105B Peter Kiewit Institute, 1110 South 67th Street, Omaha, NE 68182-0176, USA

ARTICLE INFO

Keywords:
Shear pocket connection
Composite section
Precast
Bridges
Full-depth deck panel

ABSTRACT

Current bridge design codes do not provide adequate criteria/procedures for designing full-depth precast concrete deck systems, especially those with shear pocket connections. Instead, these systems and their connections are designed on a case-by-case basis by either conducting necessary testing or adopting the design criteria/procedures developed primarily for cast-in-place concrete deck systems. Shear pocket connections formed using steel hollow structural sections (HSS) provide a promising solution to connecting precast concrete deck panels to the supporting girders due to their superior structural performance and simplicity of panel fabrication. The main objective of this paper is to develop criteria/procedures for designing HSS formed shear pocket connections in full-depth precast concrete deck systems. These procedures will assist bridge designers in selecting pocket dimensions, HSS thickness, pocket anchorage and reinforcement necessary to maximize the connection capacity while allowing adequate construction tolerance. Experimental investigation (push-off testing) and finite element analysis (FEA) were performed to validate the developed design criteria/procedures. Analysis and testing results indicated that the developed design criteria/procedures for HSS formed shear pocket connections are satisfactory.

1. Introduction

Full-depth precast concrete deck systems is one of the promising technologies for accelerated bridge construction (ABC) because the construction of cast-in-place concrete bridge decks is one of the most time-consuming and labor-intensive operations in bridge construction [1]. Prefabrication of concrete bridge decks offers an opportunity to significantly reduce construction duration, traffic disruption, and bridge life-cycle cost. According to the American Association of State Highway and Transportation Officials (AASHTO) Load and Resistance Factor Design (LRFD) bridge design specifications section 9.4.1, full composite action between bridge deck and supporting girders is highly recommended as it improves the superstructure stiffness and economy [2]. Full-depth precast concrete deck panels are made composite by connecting them to the supporting girders using different types of shear connectors, such as bent bars, headed studs, or threaded rods with nuts [3]. These connectors are either embedded into the concrete girder during fabrication or welded to the top flange of steel girder before or after installing the precast concrete deck panels. Two approaches are commonly used to anchor the shear connectors into the full-depth precast concrete deck panels: (1) using longitudinal troughs (channels) in each deck panel above every girder line in case of continuous shear connectors; or (2) using isolated shear pockets in each deck panel above every girder line in case of discrete clustered shear connector. Fig. 1 shows examples of these connections that are used in bridge construction in the US, such as wedged shear pocket connections, longitudinal channel connections, and hollow structural section (HSS) formed shear pocket connections. The maximum spacing between shear connectors/pockets had been studies thoroughly in several experimental and analytical investigations conducted by [4–7]. Researchers indicated that stress concentration in the deck panel around the pocket need to be resisted by providing special confinement reinforcement, which makes the HSS formed shear pockets advantageous over other types of shear pockets as they eliminate the need for additional/special deck reinforcement.

This paper focuses on HSS formed shear pockets due to its excellent structural performance, especially for largely spaced connectors, and the simplicity it offers in panel fabrication as stay-in-place forms.

* Corresponding author.
E-mail addresses: raed.tawadrous@gmail.com (R. Tawadrous), gmorcous2@unl.edu (G. Morcous).

https://doi.org/10.1016/j.engstruct.2018.11.003
Received 8 May 2018; Received in revised form 10 October 2018; Accepted 1 November 2018
0141-0296/

Notation

$L_{e,max.}$	maximum effective embedment length of the shear connectors $L_{e,max.} = t_d - d_c - d_t$
$f_c^{'}$	concrete compressive strength of precast concrete deck panels
$f_{cp}^{'}$	concrete compressive strength of concrete inside the shear pocket and the haunch
A	longitudinal dimension of shear pocket (in the traffic direction)
a	spacing of shear connectors in the longitudinal direction
$A_{cv,min}$	minimum concrete interface shear area
A_{ht}	total area of steel to be placed within the haunch
A_{sf}	area of transverse reinforcement
A_v	area of shear connectors
b	spacing of shear connectors in the transverse direction
B	transverse dimension of shear pocket (perpendicular to the traffic direction)
b_a	distance between the two exterior shear connectors in the transverse direction (see Fig. 2a)
b_c	effective slab width, which is usually taken as the transverse girder spacing
C_t	construction tolerance that should be specified in the project specs. Practical construction tolerance for shear pockets is found in the literature to be between 2 and 4 in.
d	shear connector diameter
d_c	minimum concrete cover specified by AASHTO LRFD (2014) section 5.12.3
d_h	shear connector's head diameter
d_t	shear connector head thickness
f_{cd}	design value of concrete compressive strength
f_{ck}	characteristic value of concrete compressive strength
f_r	concrete tensile strength determined based on AASHTO LRFD (2014) section 5.4.2.6
f_y	yield strength of reinforcing bars (normally 415 MPa (60 ksi))
f_{yc}	yield strength of shear connector resisting interface shear
f_{yd}	design yield strength of reinforcement
f_{yp}	yield strength of the HSS (290 MPa (42 ksi) for round sections and 320 MPa (46 ksi) for rectangular/square section for A500 Gr. B)
h_f	length of the shear surface failure (e.g. shear surface b-b in Fig. 3)
h_P	shear pocket height
h_{sc}	height of the studs
K_1	the interaction coefficient for tensile force activated in the reinforcement or the dowels (fib MC 2010 Table 7.3-2)
K_d	ratio of the transverse tensile or compressive force to that of the applied shear force, V.
L_e	effective embedment length of the shear connectors (see Fig. 2 (sec. (A-A)) ($L_e = h_{ef}$)
m	number of columns of shear connectors (m = number of shear connectors in the longitudinal direction − 1)
n	number of rows of shear connectors (n = number of shear connectors in the transverse direction − 1)
N_{cbg}	nominal concrete breakout strength of group of anchors
N_n	nominal concrete breakout strength of individual anchor
n_s	number of shear studs to be welded on the exterior face of the HSS for anchorage
P	prestressing force applied on the shear pocket on the transverse direction
Q_s	shear strength of one shear stud
S_f	spacing between transverse reinforcement
S_t	transverse spacing center-to-center of the studs
T	the total tensile force that needs to be resisted by anchorage
t	HSS thickness
t_d	deck panel thickness
t_h	shear connector's head diameter
ν	strength reduction factor for concrete cracked in shear
V	applied shear force per pocket
V_{Ed}	design value of the applied shear stress
V_n	nominal shear force resistance per pocket
$V_{splitting}$	shear force per shear pocket that cause concrete to split
V_u	applied shear force per pocket at the ultimate level (LRFD)
θ_f	45° in the absence of more rigorous calculation (EN 1992-1-1:2004 sec 6.2.4)
Φ	strength reduction factor

Examples of bridges constructed using HSS formed shear pockets are: Live Oak Creek Bridge, TX (2008) and Kearney East Bypass Bridge in Kearney, NE (2015). Currently, bridge design codes do not provide any design criteria/procedures for this type of shear pockets. Therefore, the main objective of this research is to develop design criteria/procedures for HSS formed shear pockets in full-depth precast concrete deck systems to assist designers in selecting pocket dimensions, HSS thickness, pocket anchorage and reinforcement necessary that maximize connection capacity while allowing adequate construction tolerance. The paper is organized as follows. First, a review of the literature on the different failure mechanisms of shear pocket connection is presented. Second, the proposed design criteria/procedures are illustrated. Third, the experimental investigations conducted to evaluate the performance of the designed shear pockets are described. Fourth, the finite element analysis (FEA) performed to validated the proposed design and study the effect of design parameters is presented. Finally, research conclusions are summarized.

2. Failure mechanisms of shear pocket connection

Failure of shear connectors is the most desirable mode of failure in composite systems due to the ductile nature of steel yielding after achieving a certain amount of slippage between girder and deck components. However, in order to achieve that, failure of the surrounding concrete has to be prevented. In clustered shear connections, high concentrated loads exerted from shear connectors on the concrete slab and haunch (if exists) causing premature failure of concrete surrounding the shear connectors before the connectors develop their full strength. Different failure mechanisms are discussed as follows.

Concrete splitting in composite sections has been discussed by [8–13]. Oehlers [13] studied the effect of concrete splitting on the shear strength of shear connectors. Once concrete starts to crack, a gradual reduction in strength and stiffness of the concrete in the bearing zone (Fig. 2) of high triaxial compressive stresses occurs [14]. The concentrated load that a connector applies to a concrete slab can induce three distinct modes of cracking on the concrete slab, which are shown schematically in Fig. 2. The lateral cracks extending from the sides of the connector are caused by the ripping action of the concentrated load on the concrete slab. The extent of these cracks depends on the in-plane compressive forces in the slab [15]. Oehlers [13] concluded that these cracks have little effect on the dowel strength since they occur away from the high tri-axial compression bearing zone. However, observations of push-off tests done by Hatami [16] showed that providing longitudinal reinforcement in the haunch (close to the high bearing stresses adjacent to the shear connectors) eliminates the appearance of these cracks and increases the shear strength significantly. It has been

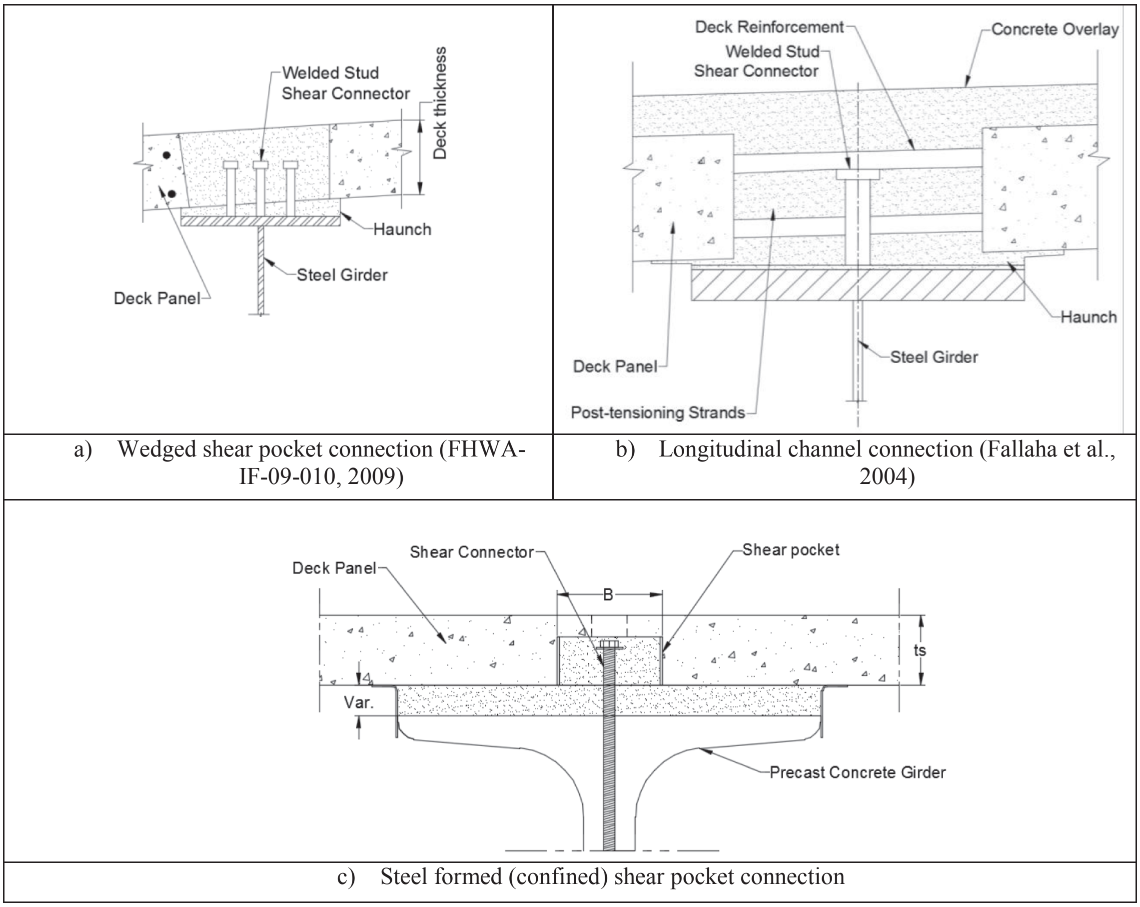

a) Wedged shear pocket connection (FHWA-IF-09-010, 2009)

b) Longitudinal channel connection (Fallaha et al., 2004)

c) Steel formed (confined) shear pocket connection

Fig. 1. Different precast concrete deck-to-girder connections.

also observed that the transverse reinforcement does not prevent splitting, instead it does limit the propagation of cracks [17]. It is worth noting that the solution of lateral stress dispersal due to concentrated load problem was first developed by Flamant [18].

For longitudinal shear failure, deck panel and girder can be idealized as flange and web, respectively, where the horizontal shear strength of the flange is analyzed as a system of compressive struts combined with ties in the form of tensile reinforcement [19], as shown in Fig. 2. In Fig. 2a, the compressive struts are represented as arrow marked “C” and the tie is represented as a tension member marked “T”. In-plane rotation of the struts of concrete stresses the transverse reinforcement in tension causing failure when this reinforcement yields or the struts crushes. Transverse reinforcement is usually placed in the slab to resist the rotation of concrete struts and hence prevents failure due to inclined shear [20]. The design equations are similar to those for stirrups in concrete beams. Eurocode 4 [21] section 6.6.6 specifies transverse reinforcement in the concrete slab to be designed to prevent premature longitudinal shear failure or longitudinal splitting. The design longitudinal shear stress for any potential surface of longitudinal shear failure within the slab shall not exceed the design longitudinal shear strength of the shear surface considered. Where the design longitudinal shear strength is given by [19] section 6.2.4(4). Fig. 3 shows typical potential shear failure surfaces to be checked, suggested by the Eurocode 4-2 [21]. Where the length of the shear surface b-b shown in Fig. 3 should be taken as equal to $2h_{sc}$ (where h_{sc} is the height of the studs) plus the head diameter for a single row of stud shear connectors or staggered stud connectors, or as equal to $(2h_{sc} + S_t)$ (where S_t is the transverse spacing center-to-center of the studs) plus the head diameter for stud shear connectors arranged in pairs.

The shear strength of shear connectors in push-off tests is greatly influenced by axial force exerted on the shear connectors due to shear friction action and/or applied tension (that may be applied accidentally during the test) that may cause concrete breakout failure. It is worth noting that most design specification provisions of interface shear are based on push-off experiments. Teraszkiewicz [22] observed that the strength of push-off tests, in which the base of push-off specimen is free to slide, is substantially less than that in push-off tests in which the base is fixed (refer to standard push-out test in British Standards [23] Section 5.3.2.4 for test configuration). Teraszkiewicz recorded reduction in shear strength of headed studs up to 50 percent when both sides were free to slide [24]. This reduction in shear strength is due to the change in the resultant axial force across the interface from compression when the base is fixed to tension in the studs, when the base is free to slide. The applied axial tensile load to the shear connectors can cause the concrete surrounding the connectors to breakout forming a cone, as shown in Fig. 2. This type of failure can be prevented by increasing the embedment length of the connectors in order to develop the yield strength of the shear connectors' material or a maximum of 415 MPa (60 ksi), as recommended by ACI 318-14 [25] (section 22.9.1.4) and AASHTO LRFD [2] (section 5.8.4.1). However, the Canadian standards [26] (section 8.9.5.4) and the European standards [19] (section 6.2.5) specify the development of the yield strength without a maximum value. Extending the shear connectors in order to achieve the development length is impractical in the case of shear pocket connections provided in the precast concrete deck. Instead, headed shear connectors or 180-degree hook for steel rebars are used.

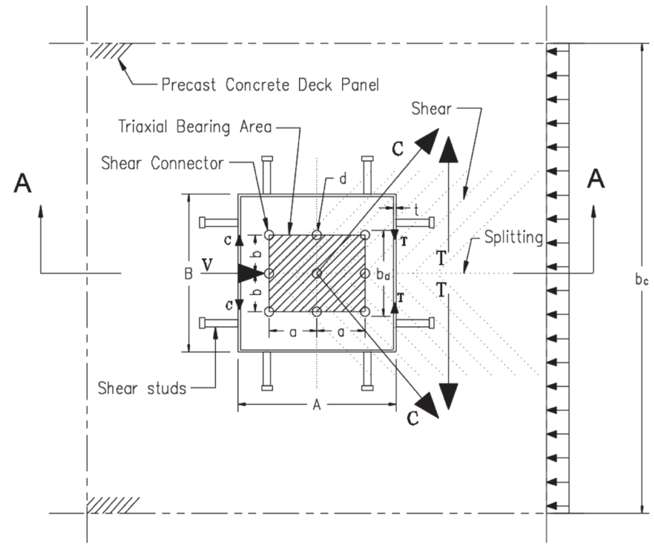

a) Plan view of shear pocket showing splitting cracks

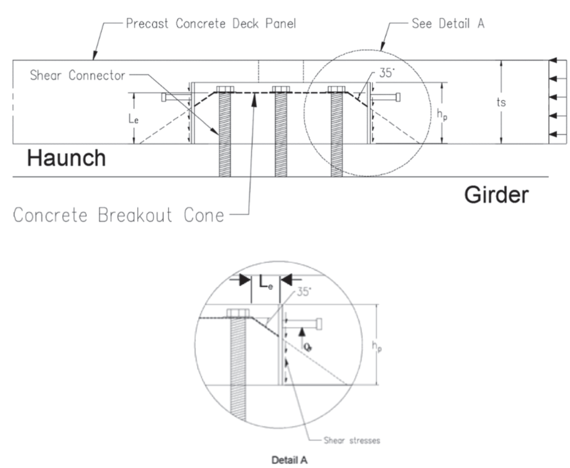

b) Concrete breakout and anchorage mode of failure

Fig. 2. Different modes of failure.

3. Proposed design procedure of shear pocket connection

Fig. 4 shows a flowchart that illustrates a general design procedure for a full-depth precast concrete deck system with shear pocket connections. This follows the traditional procedures of bridge superstructure design; however, design of shear pocket was added and design iterations are made if needed. Fig. 5 shows a flowchart that illustrates detailed design procedure for HSS-formed shear pocket connections. Four distinct modes of failure are checked and criteria were proposed to determine the following outcomes:

- Shear pocket dimensions
- HSS thickness
- Haunch reinforcement (if applicable)
- HSS anchorage (studs or bars).

3.1. Shear pocket dimensions

After designing the shear connectors using interface shear resistance provisions, the number of shear connectors, shear connector diameter, and shear connector head diameter will be known. Shear connector layout inside the shear pocket can be determined based on girder type, flange width, and skew angle (if existing). Fig. 2 shows a general shear connectors/shear pocket configuration for a clustered shear connection that has nine shear connectors. Standard HSS section is used as a shear pocket, which can be found in the American Institute of Steel Construction manual [27] Tables 1-11 through 1-13. The selection criteria of the HSS cross section should be based on finding the best fit with consideration to allow adequate construction tolerance as the minimum dimensions. Eqs. (1) and (2) present simple formulas for calculating the lower limits of shear pocket dimensions considering the distance between two exterior shear connectors and specified construction tolerance that may differ from one project to another.

$$A \geq a \cdot (m-1) + d_h + C_t \quad (1)$$

$$B \geq b \cdot (n-1) + d_h + C_t \quad (2)$$

where

A = longitudinal dimension of shear pocket (in the traffic direction) (see Fig. 2)
B = transverse dimension of shear pocket (perpendicular to the traffic direction) (see Fig. 2)
a = spacing of shear connectors in the longitudinal direction
b = spacing of shear connectors in the transverse direction
m = number of shear connectors in the longitudinal direction
n = number of shear connectors in the transverse direction
d_h = shear connector's head diameter
C_t = construction tolerance that should be specified in the project specifications. Practical construction tolerance for shear pockets is found in the literature to be between 2 and 4 in.

A preliminary HSS thickness should be selected, which will be checked later when calculating concrete splitting strength. It should be noted that standard HSS are referred to in this context because of their availability and economy, however, built-up sections or bent plates can be used as shear pockets. Upper limits for shear pocket dimensions should be determined according to the concrete splitting and concrete breakout mode of failure, which is discussed in detail in the following sections.

3.2. Concrete splitting

The splitting resistance of concrete decks without transverse reinforcement should be checked first using Eq. (3). This equation is derived based on research findings of Flamant [18]; Johnson and Oehlers [17]; and Oehlers and Bradford [24] with minor modifications to incorporate the tensile concrete strength specified by AASHTO LRFD and the prestressing effect (if exist). Prestressing effect on splitting resistance is added to the splitting equation to account for the effect of transverse prestressing force (perpendicular to the traffic direction), which exist in pretensioned precast concrete deck panels.

$$V_{splitting} = \frac{1.8 \cdot d \cdot f_r \cdot A}{2K_d} + \frac{p}{2} \quad (3)$$

where

$$K_d = \frac{1}{\pi}\left(1 - \frac{b_a}{b_c}\right)^2$$

$$b_a = b \cdot (n-1) + d$$

$V_{splitting}$ = shear force per shear pocket that cause concrete to split
K_d = ratio of the transverse tensile or compressive force to that of the applied shear force, V.
d = connector diameter

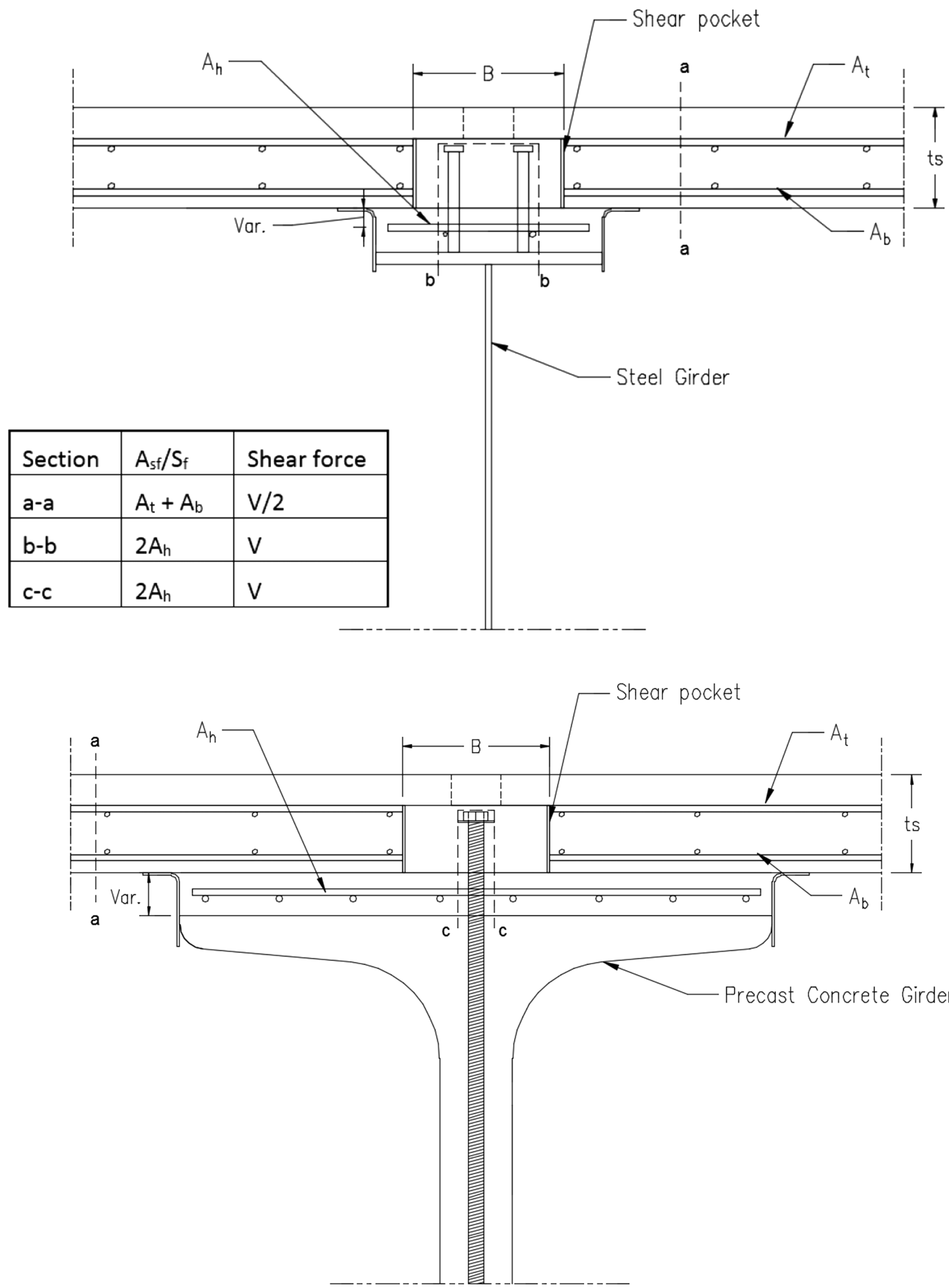

Section	A_{sf}/S_f	Shear force
a-a	$A_t + A_b$	V/2
b-b	$2A_h$	V
c-c	$2A_h$	V

Fig. 3. Typical potential shear failure surfaces using concrete and steel girders.

f_r = concrete tensile strength determined based on AASHTO LRFD [2] section 5.4.2.6 using f'_{cp}, where f'_{cp} is the concrete compressive strength of concrete inside the shear pocket and the haunch.
b_a = distance between the two exterior shear connectors in the transverse direction (see Fig. 2a)
b_c = effective slab width, which is usually taken as the transverse girder spacing
P = prestressing force applied on the shear pocket on the transverse direction.

When the applied shear force per pocket (V) is less than the splitting resistance ($V_{splitting}$), then, minimum thickness available for the chosen HSS should be used. Otherwise, required HSS thickness should be calculated using Eq. (4). Johnson and Oehlers [17] assumed that the reduction in shear connector forces due to bond and friction is negligible,

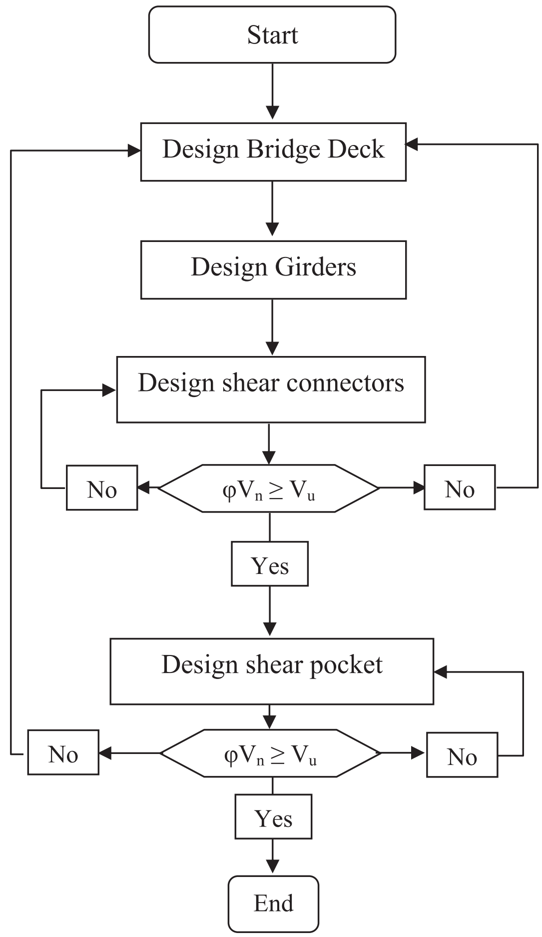

Fig. 4. Flowchart of general design procedures for full-depth precast concrete deck systems with shear pocket connections.

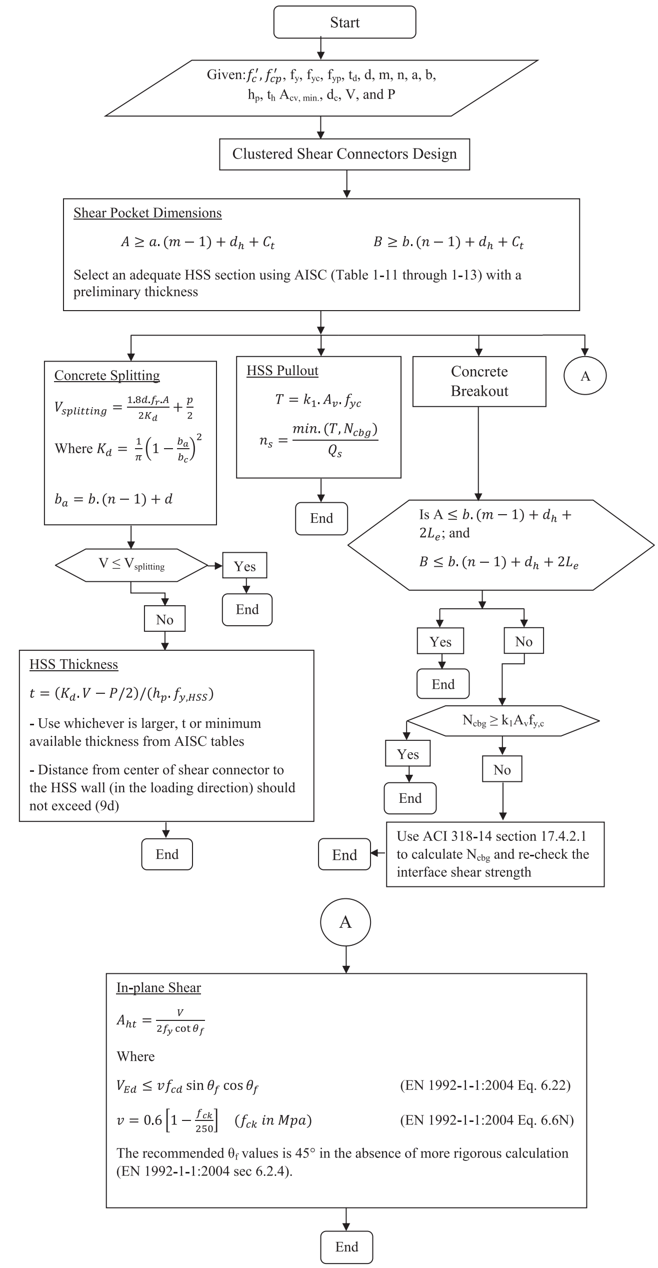

Fig. 5. Flowchart illustrating design procedures of shear pocket connection.

which is also maintained in this study.

$$t = (K_d V - P/2)/(h_p \cdot f_{yp}) \tag{4}$$

where

V = applied shear force per shear pocket
f_{yp} = yield strength of the HSS (290 MPa (42 ksi) for round sections and 320 MPa (46 ksi) for rectangular/square section for A500 Gr. B)
h_p = shear pocket height
t = HSS thickness.

Eurocode 4 [21] section 6.6.4 provides special provisions for shear connectors that cause splitting and specifies limits on transverse reinforcement location to be considered effective in resisting splitting forces. This limit is taken as (*9d*) from the center of the shear connectors to the tension side of the HSS. This requirement should be considered to adequately size the pocket to effectively resist splitting forces due to the application of concentrated forces in the longitudinal direction.

3.3. In-plane shear (longitudinal shear)

In order to prevent concrete failure in tension in the haunch zone, concrete zone between top flange of the girder and the soffit of precast panel, transverse reinforcement needs to be added to resist tensile force and to achieve equilibrium of the strut and tie system. Due to construction requirements of bridges, the haunch height may vary from 50 to 152 mm (2–6 in.) to accommodate girder's camber [16]. Therefore, concrete shear strength of the haunch zone, specifically the area within the shear pocket, is of primary importance to prevent premature longitudinal shear failure. This area of the haunch experiences high concentrated shear stresses from the shear connectors. Eurocode design provision, [19] section 6.2.4(4) (Eq. (5)), is adopted for calculating the required shear reinforcement.

$$(A_{sf} \cdot f_{yd}/s_f) \geq V_{Ed} \cdot h_f/\cot\theta_f \tag{5}$$

Table 1
Push-off experimental plan.

Group	Specimen type and size	Shear connector type and size	Shear pocket type and size	f_c (haunch/pocket)	No. of specimens
A	Concrete Block 6 ft long 3′ 4″ × 2′ 6″	1.5″ A193 B7 Threaded Rod	Round HSS 7.5 × 0.188	7.6 ksi SCC	2
B	Concrete Block 6 ft long 3′ 4″ × 2′ 6″	1.5″ A193 B7 Threaded Rod	Round HSS 10 × 0.188	7.6 ksi SCC	2
C	Concrete Block 6 ft long 3′ 4″ × 2′ 6″	1.5″ A193 B7 Threaded Rod	Round HSS 10 × 0.25	7.5 ksi SCC	2
D	Concrete Block 6 ft long 3′ 4″ × 2′ 6″	1.5″ A193 B7 Threaded Rod	Round HSS 12.75 × 0.25	6.5 ksi SCC	2
E	Concrete Block 6 ft long 3′ 4″ × 2′ 6″	1.5″ A193 B7 Threaded Rod	Round HSS 14 × 0.25	7.5 ksi SCC	2
F	Concrete Block 8 ft long 3′ 4″ × 2′ 6″	2–1.25″ A193 B7 Threaded Rod	Rec. HSS 16 × 12 × 5/16	9.6 ksi Grout	3
G	Steel Girder 8 ft long W30 × 173	6 - 1″ Type B Studs	Rec. HSS 16 × 12 × 5/16	10 ksi Grout	3

Note: 1 in. = 25.4 mm; 1 ft = 305 mm; 1 ksi = 6.9 MPa.

where

$V_{Ed} \leq v \cdot f_{cd} \cdot \sin\theta_f \cdot \cos\theta_f$
$v = 0.6\left[1 - \frac{f_{ck}}{250}\right](f_{ck} \text{ in MPa})$
A_{sf} = area of transverse reinforcement
S_f = spacing between transverse reinforcement
V_{Ed} = design value of the applied shear stress
f_{cd} = design value of concrete compressive strength
f_{ck} = characteristic value of concrete compressive strength
f_{yd} = design yield strength of reinforcement
h_f = length of the shear surface failure (e.g. shear surface b-b in Fig. 3)
v = strength reduction factor for concrete cracked in shear
θ_f = 45° in the absence of more rigorous calculation [19] (sec 6.2.4).

Total area of steel to be placed in the haunch (A_{ht}), which correspond to critical section b-b or c-c in Fig. 3, can be calculated by Eq. (6):

$$A_{ht} = \frac{V}{2f_y \cdot \cot\theta_f} \tag{6}$$

where

f_y = specified yield strength of the reinforcing bars.

3.4. Concrete breakout

Concrete breakout strength can be calculated using ACI 318-14 [25] provisions section 17.4.2 where the strength of group of connectors is the summation of individual connector strength in case the connectors are spaced three times the embedment depth or more, which is not likely to occur when using clustered shear connectors. In case of closely spaced shear connectors in clustered shear connections, the group strength will control the design. In addition, the specified yield strength of the shear connectors will be difficult to achieve, especially when using high strength shear connectors (greater than 415 MPa (60 ksi)). Recent experimental investigations on interface shear [28–31,16] showed that the measured connector strains were less than the yield strain. The mean value of the strain, irrespective to the surface roughing condition, was approximately 50 percent of the yield strain of the connectors [29]. A more accurate interface shear model was developed by Randi [32], which is adopted by *fib* Model code 2010 [33] and can be used in calculating the axial tensile force that needs to be developed when checking the concrete breakout [3,29]. This force corresponds to the clamping effect exerted on the shear connectors due to shear friction. Eq. (7) shows the tensile force that need to be developed to prevent concrete breakout. It is worth noting that the general assumption of ductile connection is valid, even though, the measured connector strains by different researchers [28–31,16] was less than the yield strain. This is attributed to the fact that strain is usually measured at a single point on the connector, which does not reflect the behavior of the connector under ultimate loads. Connectors resist interface shear by clamping the components and by the dowel action, which is a ductile behavior that results in bending the shear connectors. For more information about the shear connector behavior, please refer to Ref. [3].

$$T = k_1 \cdot f_{yc} \cdot A_v \tag{7}$$

where

T = total tensile force that needs to be resisted
k_1 = interaction coefficient for tensile force activated in the reinforcement (fib MC 2010 Table 7.3-2). k_1 = 0.5 for roughened interface and zero for smooth interfaces (i.e., interface with steel). The surface is considered to be roughened when the peak-to-mean surface roughness amplitude is larger than or equal to 1.5 mm (0.06 in.) [33].
f_{yc} = yield strength of shear connector resisting interface shear
A_v = total area of shear connectors.

Historically, the most common anchor reinforcement used in resisting concrete breakout in tension is a U-shape (hairpins) in the direction of the applied tensile force [25]. ACI 318-14 [25] section 17.4.2.9 denotes that the design strength of the anchor reinforcement shall be permitted to be used instead of the concrete breakout strength in determining anchor capacity. Only reinforcement spaced less than half the embedment depth from the anchor centerline should be included as anchor reinforcement considering that reinforcement is fully developed in both areas.

Cannon et al. [34] recommended using U-shape hairpins for direct force transfer to be placed at the potential breakout cone symmetrically within 1/3 of the embedment depth from the edge of the anchor head. Lee et al. [35] observed the effectiveness of placing anchorage reinforcement closer to the anchor on the tension capacity throughout his tests. Similarly, CEB [36] design guidelines recommend using anchorage reinforcement in form of U-shape within the breakout cone at a distance of no more than half the embedment depth from the anchor centerline, which agrees with ACI 318-14 [25]. The effective range is increased in CEN/TS (by the European Committee for Standardization) to ¾ of the embedment depth. CEB [36] allows stirrups in beams within

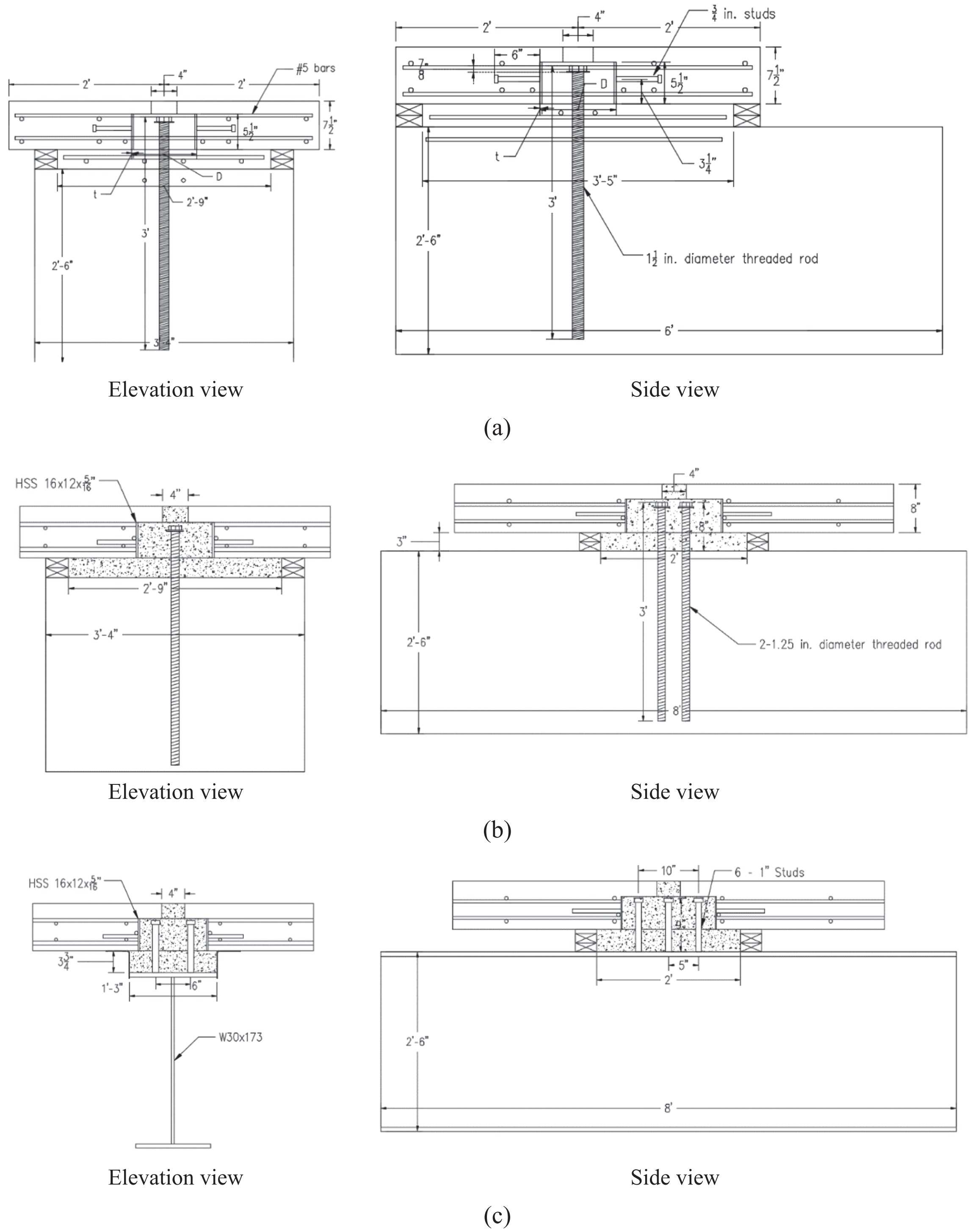

Fig. 6. Typical views for push-off specimens of: (a) groups A, B, C, D, and E; (b) group F; and (c) group G (1 in. = 25.4 mm; 1 ft = 305 mm).

one embedment depth from the anchor centerline to be used as anchor reinforcement.

The tension reinforcement provisions in most design codes of practice are based on the assumption that concrete breakout failure cone forms first before reinforcement located within a certain range from the anchor bolt carry the tension force. The usage of the HSS as anchor reinforcement in tension (in the vertical direction) is employed to prevent brittle concrete breakout failure. A maximum distance from the edge of the head of the outer shear connector to the nearest HSS wall of 1.0 L_e (one effective embedment length) is adopted in determining the upper limits of shear pocket dimension as shown in Fig. 2. Eqs. (8) and (9) present simple formulas for calculating the upper limits of the proposed shear pocket dimension in the longitudinal and transverse directions respectively. The recommended limits are verified in this study through experimental investigations, which is discussed in the following sections. Concrete breakout strength should be check only

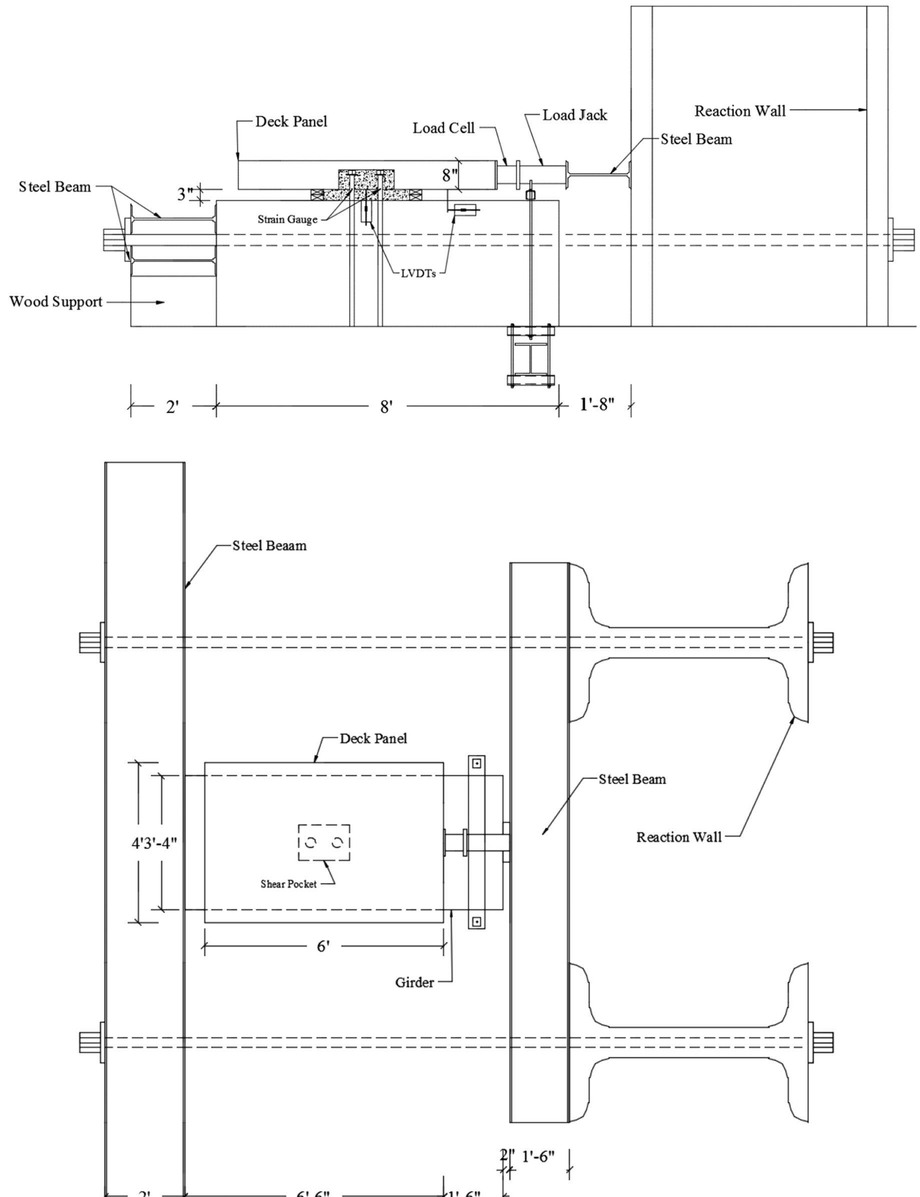

Fig. 7. Push-off test setup (elevation and plane view) (1 in. = 25.4 mm; 1 ft = 305 mm).

if the maximum recommended shear pocket dimensions are exceeded. ACI 318-14 [25] section 17.4.2 provision should be used in calculating the concrete breakout strength of the clustered shear connectors inside the shear pocket and shear connectors strength should be re-calculated.

$$A \leq b\cdot(m-1) + d_h + 2L_e \tag{8}$$

$$B \leq b\cdot(n-1) + d_h + 2L_e \tag{9}$$

where

L_e = effective embedment length of the shear connectors (see Fig. 2 - Detail A), where maximum $L_e = t_d - d_c - d_t$.

3.5. Anchorage design of shear pocket

In order to achieve anchorage between the HSS and deck panel, anchors are designed to resist the smaller of tension force exerted from clamping forces due to shear friction or the breakout force. Shear connectors (studs or bars) are welded to the exterior surface of the HSS as shown in Fig. 2. Deck transverse and longitudinal reinforcement are recommended to be placed underneath the welded studs or bars in order to prevent concrete spalling in case if the bottom transverse deck reinforcement is widely spaced. The number of shear studs can be calculated by Eq. (10), and the T value is given by Eq. (7):

$$n_s = \frac{Min\cdot(T \quad or \quad N_{cbg})}{Q_s} \tag{10}$$

where

n_s = number of shear studs to be welded on the exterior face of the HSS for anchorage
Q_s = shear strength of one shear stud
N_{cbg} = nominal concrete breakout strength of group of anchors.

4. Experimental investigation

Table 1 shows the plan of the experimental investigation that includes testing 16 push-off specimens. This plan was designed to validate the recommended minimum and maximum shear pocket dimensions, HSS thickness, and haunch reinforcement. Specimens “A” through “E” focused on investigating the validity of the proposed design procedures/criteria using round HSS and one large-diameter shear connector. Specimens “F” and “G” focused on studying the behavior of rectangular HSS with clustered shear connectors on concrete and steel girders. Table 1 lists specimen type and dimensions; shear connector type, number, and size; shear pocket dimensions and thickness; measured concrete compressive strength; and number of specimens.

4.1. Push-off specimens details

Fig. 6 shows dimensions and reinforcement details of push-off specimens. For all the specimens, the girder top surface was roughened with at least 6 mm (0.25 in.) amplitude and cleaned prior to placing deck panel and the interface shear area was considered to be the area of monolithic concrete at the deck soffit, which is the area of the shear pocket. Both haunch and shear pocket were filled with 42 MPa (6 ksi) self-consolidating concrete (SCC) in specimen groups A to E and 62 MPa (9 ksi) non-shrink grout in specimen groups F and G. Table 1 also lists the measured concrete/grout compressive strength for each group. All deck panels had top and bottom reinforcement used for typical cast-in-place concrete bridge decks. Shear pockets were formed using hollow steel structural sections (HSSs) placed at the centroid of deck panels. The height of all shear pockets was 140 mm (5.5 in.) and the minimum deck thickness was 190 mm (7.5 in.) to ensure adequate cover thickness. The shape and plan dimensions of the HSS were variables. Shear studs were welded to the HSS in specimens in groups A through E and steel bars (#5) were welded to the HSS in specimens in group F and G for anchorage. Properties of the HSS used in shear pockets are as follows: ASTM A500 Gr. B with yield strength F_y = 290 MPa (42 ksi) for round HSS and F_y = 320 MPa (46 ksi) for rectangular HSS, and tensile strength F_u = 400 MPa (58 ksi).

4.2. Push-off test setup

Fig. 7 shows the test setup and instrumentation of the push-off test, which consists of the following:

- Supporting frame: Two horizontal threaded rods anchored to the reaction wall from one side and to a horizontal steel beam at the other side.
- Tie-down steel frame anchored to the floor to prevent the specimens' rotation.
- Hydraulic Jack, load cell, and loading plates.
- LVDTs (Linear Variable Differential Transformer) to measure relative movements.

A horizontal load was applied to the center of the deck panel using 400-kip hydraulic jack, load cell, and spreader beam as shown in Fig. 7. The load was applied gradually at a rate of approximately 4 kips/sec. until the ultimate shear resistance of the interface shear was reached. The specimens were loaded at this loading rate based on successfully tested specimens found in the literature [6] for similar specimens. The relative displacements between the supporting girder and deck panel were measured in both horizontal and vertical directions using LVDTs. The load-displacement relationships of the tested specimens were recorded using data acquisition system for analysis.

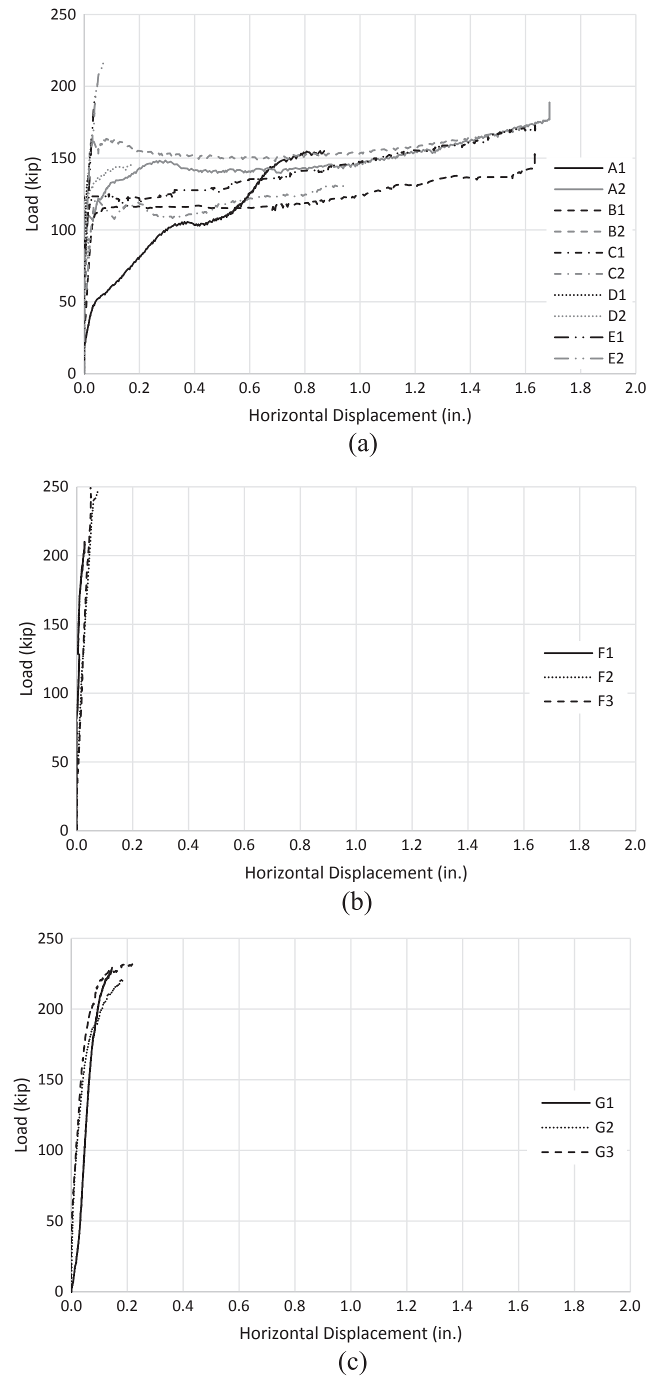

Fig. 8. Load vs horizontal displacement relationships of: (a) group A, B, C, D, and E; (b) group F; and (c) group G (1 in. = 25.4 mm; 1 kip = 4.448 kN).

4.3. Push-off experimental test results

Fig. 8 shows the load versus horizontal displacement for the sixteen push-off specimens. The plot is divided into three sets to compare results of similar shear pocket connections: First set (a), shows the behavior of specimens in groups A, B, C, D and E; second set (b), shows the behavior of specimens in group F; and third set (c), shows the behavior of specimens in group G. Fig. 8a shows that specimens of groups A, B, and C experienced significant horizontal displacement as the load

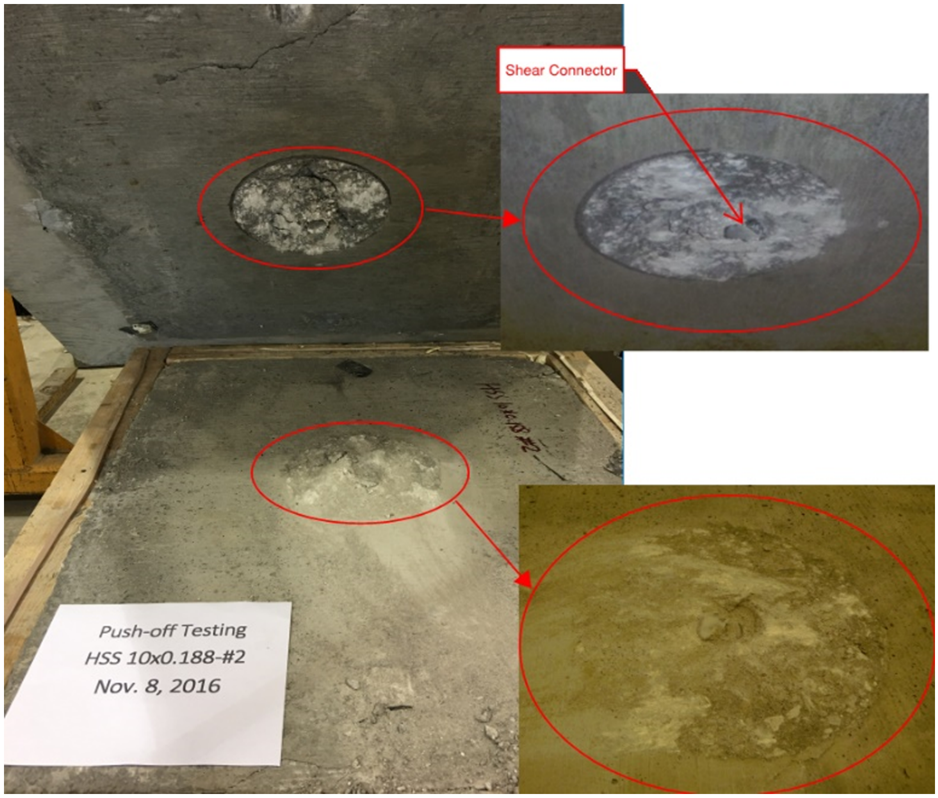

Fig. 9. Mode of failure for specimens A2, B1, B2, and C1.

Fig. 10. Mode of failure for specimens A1, C2, D1, D2, E1, and E2.

increased and the connectors sheared off in four out of six tests, as shown in Fig. 9. The horizontal displacement at failure in these specimens ranged from 0.9 to 1.6 in. However, specimens in groups D and E showed less horizontal displacement and failed by breakout of pocket concrete, as shown in Fig. 10 at displacement of less than 0.1 in. All six

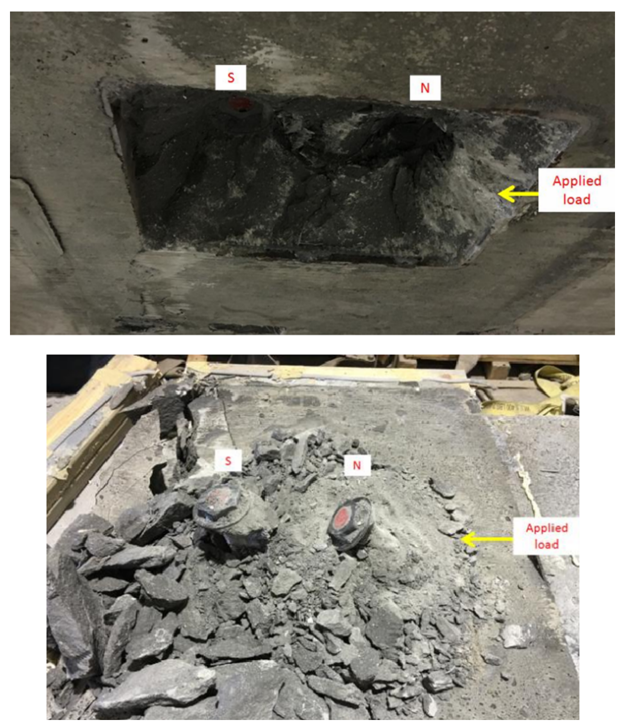

Fig. 11. Mode of failure for specimens F1, F2, and F3.

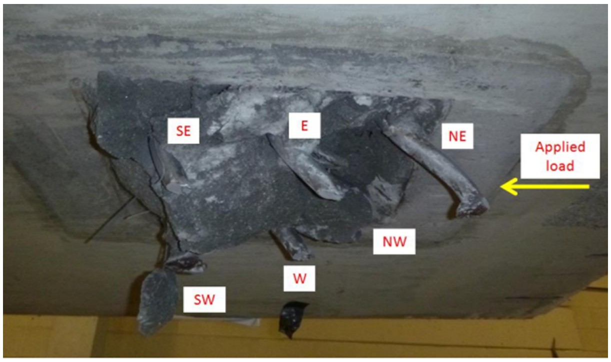

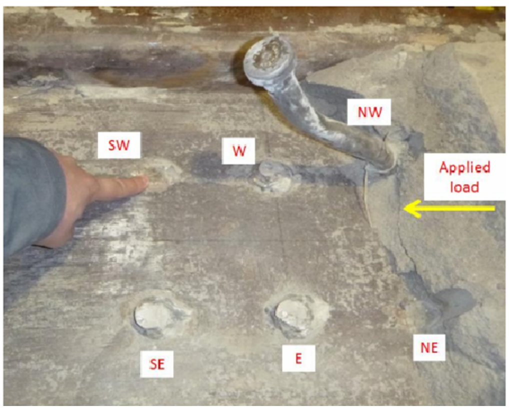

Fig. 12. Mode of failure for specimens G1, G2, and G3.

specimens in groups F and G showed similar behavior (see Figs. 11 and 12). The displacement at failure was recorded to be slightly less than 0.1 in. for specimens in group F and approximately 0.2 in. for specimens in group G. Same grout material was used for groups F and G, however, the shear connectors type was different. For more detailed experimental results, refer to Tawadrous [37] and Tawadrous and Morcous [3].

In general, load-displacement curves showed three distinct behaviors: First, linear behavior up to a very small displacement (0.01 in.), which defines the cohesion and aggregate interlocking failure of concrete at the interface [38]. Second, linear behavior up to a tangible but limited displacement (0.1 in.), which defines the shear friction failure. Third, the nonlinear behavior, where significant displacement was observed with a slight increase in the load resistance by the connection until shear connectors were sheared off. The main contributor to load resistance in this phase is dowel action of the connector, where the shear connectors were bent significantly and excessive displacement was recorded. Specimens of groups A through C experienced the three phases before failure. However, specimens of groups D and E experienced only the first two phases and did not experience the post yielding behavior and the failure was sudden. Similarly, specimens of groups F and G experienced brittle failure, where the post yielding behavior was not achieved and the failure mode included concrete crushing in the haunch area as shown in Figs. 11 and 12, respectively. Table 2 lists detailed testing results of the sixteen push-off specimens including the measured concrete compressive strength of the haunch and the shear pocket at testing time; shear pocket dimensions; measured and predicted interface shear strength; and mode of failure.

Failure mode is significantly affected by the shear pocket confinement and haunch reinforcement that could be clearly seen in Fig. 8 when comparing load-displacement curves of all the specimens. Shear pocket confinement by HSS was deemed to provide adequate confinement and development for the connectors in group A, B, and C, however, confinement of specimens in groups D and E was not effective as the diameter gets bigger. All specimens in groups A to E contained haunch reinforcement, while specimens in groups F and G did not, which resulted in brittle failure of grout in the haunch area.

Examining measured failure loads for each group that composed of two identical specimens showed high test result variabilities ranging from 11.7% to 31.8% in groups E and C, respectively. Studying previous experimental push off test results conducted by Wallenfelsz [39], Badie et al. [6], and Hatami [16] shows that such a high variability is not uncommon.

Table 2
. Summary of push-off test results.

Specimen ID	f_c (ksi)	Pocket dimensions	V_{test} (kips)	$V_{predicted}$ (kips) (*fib*)	$V_{predicted}$ (kips) (AASHTO)	Mode of failure
A1	7.30	HSS 7.5 × 0.188	155.0	67.4	59.9	The Connector was bent. Concrete crushing in the shear pocket
A2	7.80	HSS 7.5 × 0.188	188.8	70.4	59.9	The connector sheared off. No concrete damage was observed inside the shear pocket nor the haunch
B1	7.30	HSS 10 × 0.188	152.8	116.9	109.1	The connector sheared off. No concrete damage was observed inside the shear pocket nor the haunch
B2	7.80	HSS 10 × 0.188	176.5	118.2	109.1	The connector sheared off. No concrete damage was observed inside the shear pocket nor the haunch
C1	7.50	HSS 10 × 0.25	173.1	117.2	106.4	The connector sheared off. No concrete damage was observed inside the shear pocket nor the haunch
C2	7.50	HSS 10 × 0.25	131.3	117.2	106.4	The Connector was bent. Concrete crushing in the shear pocket
D1	6.5	HSS 12.75 × 0.25	163.2	81.4	97.9	The Connector was bent. Concrete crushing in the shear pocket
D2	6.5	HSS 12.75 × 0.25	145.3	81.4	97.9	The Connector was bent. Concrete crushing in the shear pocket
E1	7.50	HSS 14 × 0.25	196.3	87.42	108.4	The Connector was bent. Concrete crushing in the shear pocket
E2	7.50	HSS 14 × 0.25	219.3	87.42	108.4	The Connector was bent. Concrete crushing in the shear pocket
F1	6.30	HSS 16 × 12 × 5/16	210.0	164.7	233	Connectors were bent. North connector was bent more and hit the south connector. Grout crushing in the haunch
F2	10.80	HSS 16 × 12 × 5/16	247.8	182.2	233	The north connector was pulled out of the concrete girder
F3	8.30	HSS 16 × 12 × 5/16	249.2	173.1	233	Connectors were bent. Grout crushing in the haunch
G1	6.20	HSS 16 × 12 × 5/16	229.3	171.33 277.25^{+}	187.37 282.6*	5 Studs were sheared off. Grout crushing in the haunch
G2	9.10	HSS 16 × 12 × 5/16	221.4	191.4 348.33^{+}	187.37 282.6*	6 Studs were sheared off. Grout crushing in the haunch
G3	9.10	HSS 16 × 12 × 5/16	232.9	191.4 338.4^{+}	187.37 282.6*	2 studs were sheared off. Grout crushing in the haunch

* Interface shear strength was calculated using AASHTO LRFD equation 6.10.10.4.3.
\+ Interface shear strength was calculated using *fib* MC 2010 equation 6.4-2. Note: 1 in. = 25.4 mm; 1 kip = 4.448 kN; 1 ksi = 6.9 MPa.

Table 3
Properties of different steel elements.

Element	ASTM Standard	f_y (ksi)	f_u (ksi)	E (ksi)
Threaded rod	ASTM A193 B7	105	125	29,000
HSS	ASTM A500 Gr. B	42	58	29,000
Bars	ASTM A-615	60	90	29,000

Note: 1 ksi = 6.9 MPa

5. Finite element analysis (FEA)

Non-linear FEA is used to investigate the behavior of the tested push-off specimens. The main goal of conducting the FEA is study the effect of other parameters, such as concrete compressive strength and shear pocket dimensions on the overall connection behavior. A commercial FEA package was used in the analysis (ANSYS 17.2 package [40]). Material models, modeling technique, geometry description, boundary conditions, and loading procedures, are discussed briefly in the following section, refer to Tawadrous [37] for a more detailed discussion. Experimental push-off tests were used to calibrate the developed finite element (FE) models to further conduct parametric study.

5.1. Modeling technique

5.1.1. Material models

Properties of the 38 mm (1.5 in.) diameter threaded rods that were used as shear connectors, HSS, and steel bars are listed in Table 3. These values were verified using coupon test results provided by the manufacturer, for each steel product, which were also used in the analysis. Fig. 13(a) shows the stress-strain relationship used for the threaded rods, steel tube, and steel reinforcement rebars. The elastoplastic uniaxial material model was used, which is provided with bi-linear kinematic hardening using Von Mises plasticity. Fig. 13(b) shows stress-strain curve used to model the concrete compressive strength in the FE model according to Badiger and Malipatil [41].

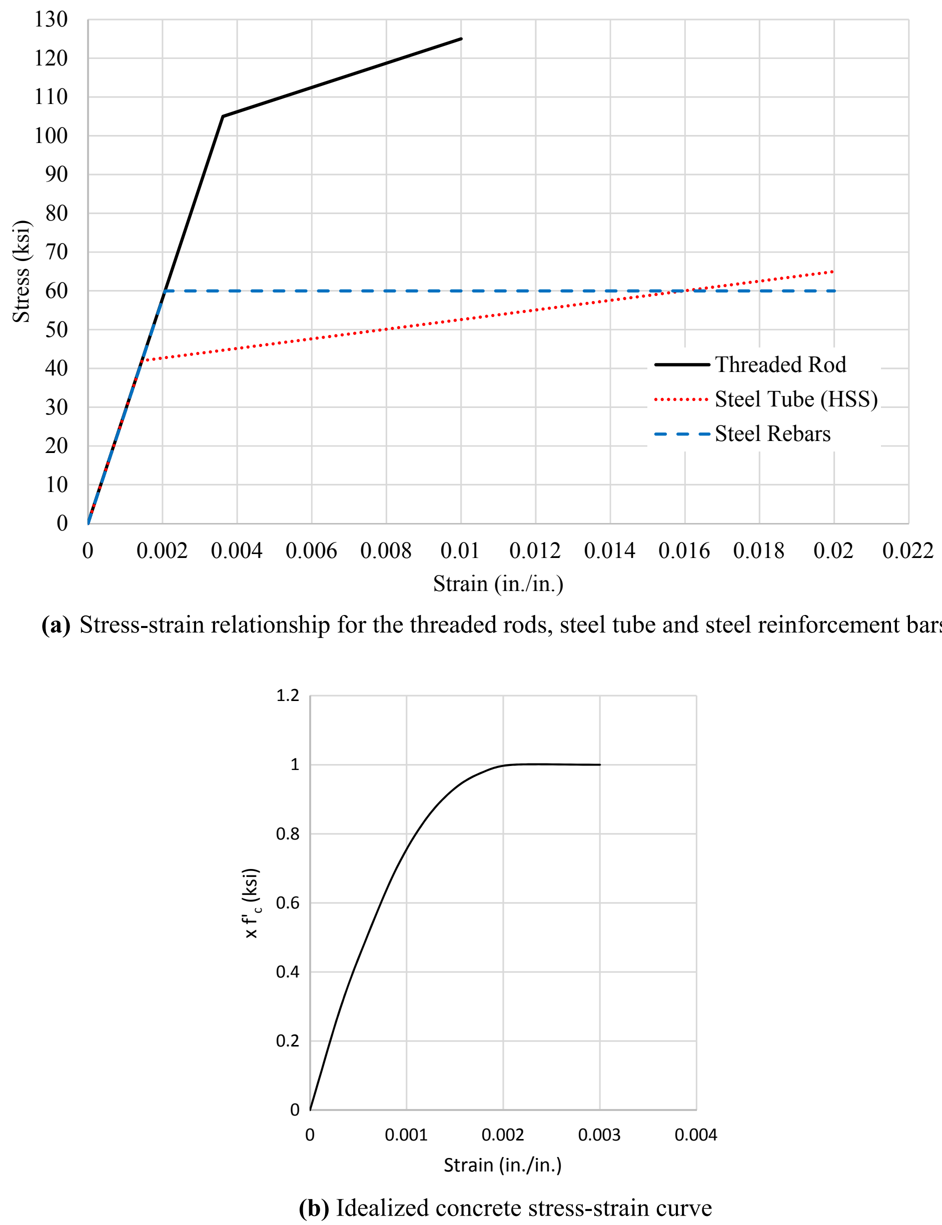

Fig. 13. Stress–strain relationship of different materials used in FEA (1 in. = 25.4 mm; 1 ksi = 6.9 MPa).

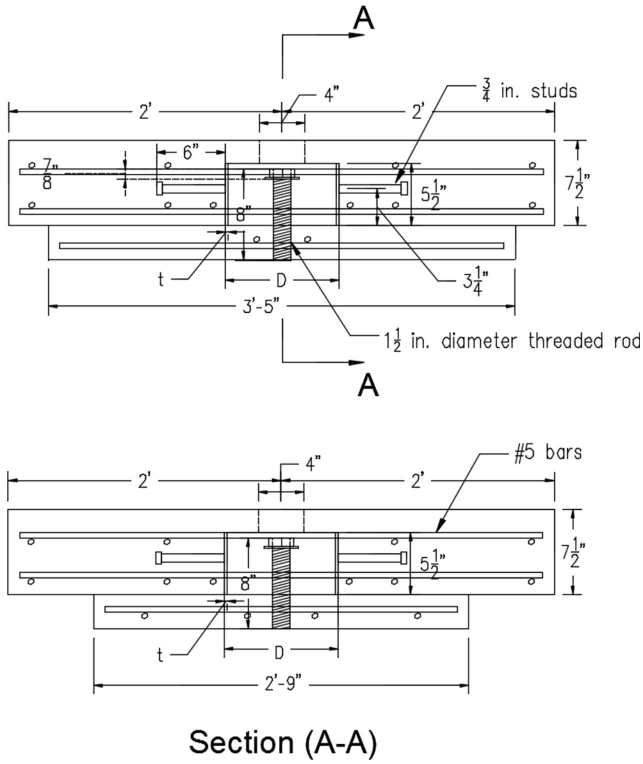

Fig. 14. Modeled part of the push-off test in FEA (1 in. = 25.4 mm; 1 ft = 305 mm).

5.1.2. Element models

Concrete was modeled by using 8-node SOLID65 element, which has three translational degrees of freedom at each node, in addition to capabilities of cracking (in three orthogonal directions) and crushing. The element has one solid material and up to three rebar materials in three directions. Thus, this element is commonly used to accommodate nonlinear material properties [40]. The steel tube section was modeled using 4-node SHELL181 element with six degrees of freedom at each node: translations in the x, y, and z directions, and rotations about the x, y, and z-axes [40]. Shear connectors (threaded rods) were modeled with smooth surface using SOLID185 element. This element is defined by eight nodes with three degrees of freedom at each node: translations in the nodal x, y, and z directions. The element has plasticity, hyper-elasticity, stress stiffening, creep, large deflection, and large strain capabilities. It also has mixed formulation capability for simulating deformations of nearly incompressible elastoplastic materials, and fully

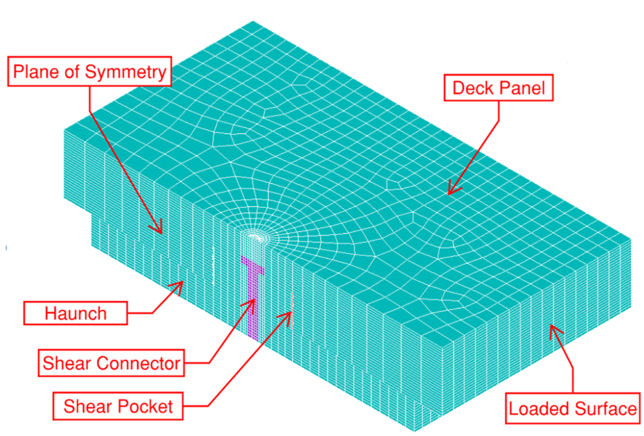

Fig. 15. Components of the FEA model.

incompressible hyper-elastic materials [40]. Shear studs and steel reinforcement rebars were modeled using LINK8 element, which is a uniaxial tension-compression element with three translational degrees of freedom at each node and no bending stiffness. Contact element was used to model the friction between different elements and dowel action of the shear connectors. Frictional contact was defined between the concrete of the shear pocket and the haunch. However, frictionless contact was used between the precast concrete deck and the haunch to prevent penetration between these two parts in the model because adhesion between soffit of precast concrete deck panel and haunch is negligible. Bonded contact element was defined between the shear connectors and the concrete for simplicity. The type of interaction between different elements, by using the contact element, in solid volumes were setup without node sharing between the adjacent elements.

5.1.3. Model geometry, boundary conditions, and loading

The push-off shear tests were modeled utilizing the symmetry function, where half the model was considered for the analysis. In order to simplify the model, the precast concrete girder was eliminated from the model and only the haunch and the precast concrete deck were considered. This simplification was justified during the experimental testing phase where the interface between the girder and the haunch did not experience any sign of damage or deformation. Therefore, a fixed boundary condition was reasonably assumed at the bottom face of the haunch. Fig. 14 shows a sketch of the modeled part of the push-off tests. Element geometric details for shear connector, concrete haunch, deck slab, and shear pocket are also described in Figs. 14 and 15. The deck slab had a dimension of 1220 mm (48 in.) by 1220 mm (48 in.) and height of 190 mm (7.5 in.). The haunch had dimensions of 1016 mm (40 in.) by 840 mm (33 in.) and a height of 75 mm (3 in.). The dimension of the shear pocket varied throughout the study; however, the height remained constant and had a value of 140 mm (5.5 in.).

Symmetric boundary conditions were applied to the surfaces of symmetry of the FE models. The soffit of the haunch was prevented from moving and rotating by applying zero translation degrees of freedom to the entire surface. Horizontal load was applied through surface displacement that was increased gradually, utilizing load-step feature, until the final failure happened at the connection.

5.2. Model calibration

In order to calibrate the FE models, specimens "A" through "E" were modeled and compared to the experimental results. Fig. 16 shows the load-horizontal displacement relationship of 10 push-off experimental tests along with the predicted load-horizontal displacement curves using FEA. All the shear pocket connections experienced two distinct behaviors except HSS 12.75x0.25 and HSS 14x0.25 specimens where only one behavior was observed. First, linear increase in the load resistance by the connection with a very small displacement increasing rate up to a point where the load-displacement curve started to change the slope. The displacement typically ranges from 0.01 in. to 0.03 in. at the end of this phase. Second, the nonlinear phase, where significant displacement was observed with a slight increase in the load resistance by the connection. HSS 12.75 × 0.25 and HSS 14 × 0.25 shear pockets achieved the first phase only, then sudden concrete breakout failure occurred and the connection was not able to achieve the dowel resistance or post-yielding resistance. This is attributed to the lack of confinement of the concrete surrounding the shear connector where both shear pocket sizes were larger than the recommended maximum shear pocket dimension limit (11.5 in.) and did not function actively as a confining reinforcement and/or tension reinforcement.

Table 4 lists the predicted (using FEA) and measured load values at yielding and ultimate levels. The measured average test results of two identical specimens were used to compare with the predicted values. The table also show the percentage error between measured and predicted values. The comparison shows an average error of 10.5% and

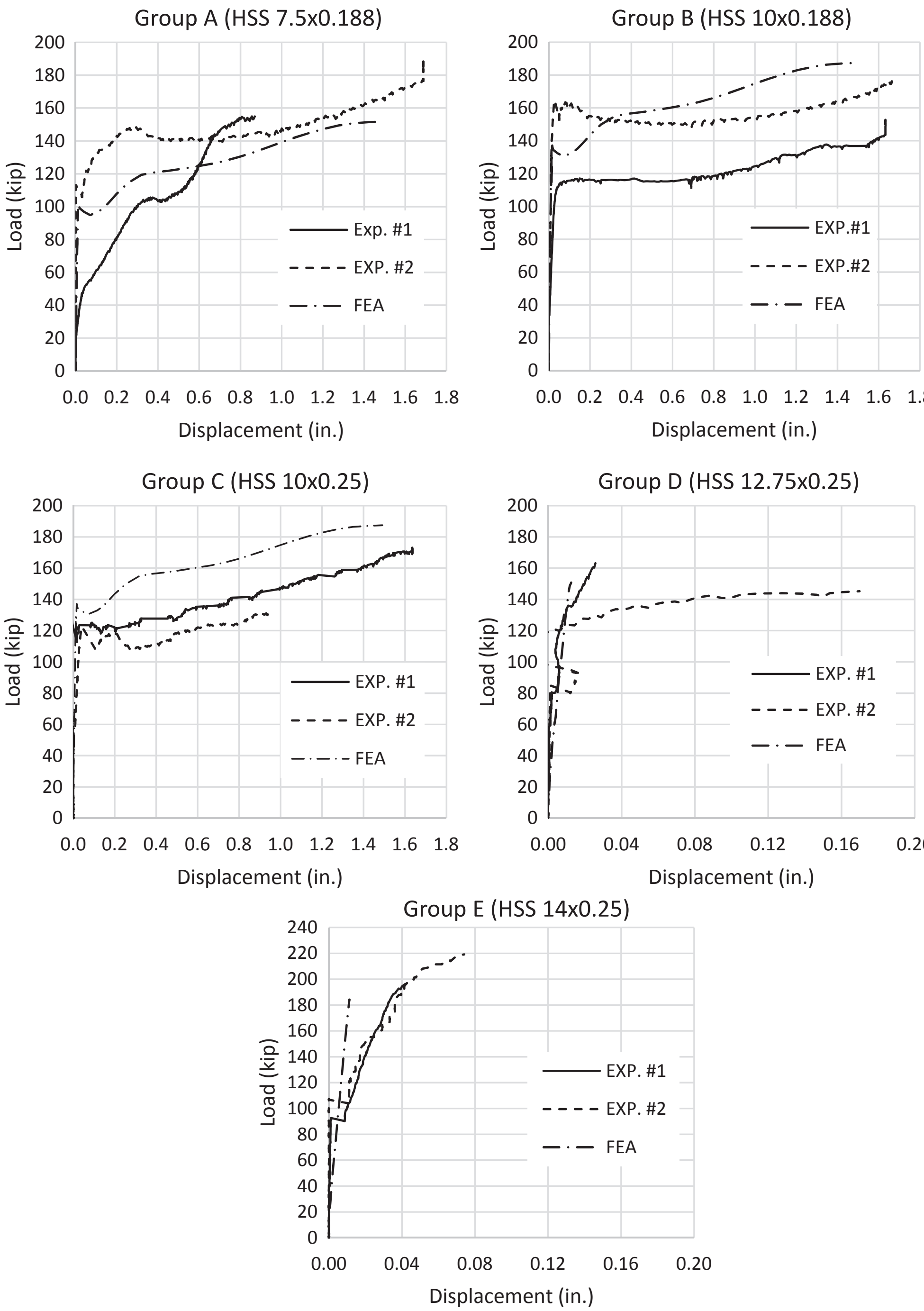

Fig. 16. Load-displacement relationships of different shear pocket sizes (1 in. = 25.4 mm; 1 kip = 4.448 kN).

12.3% at yielding and ultimate load levels, respectively. Predicted values do not match test data very well and the reason could be attributed to several parameters such as variability in support and loading conditions, concrete and steel properties, applied load eccentricity with respect to failure plane, and actual specimen dimensions. The variation between measured and predicted values should not negatively affect the conducted parametric study since the relative behavior of these parameters was studied and not the absolute behavior.

Fig. 17a shows the shear stress contours at the interface between the haunch and the deck panel at failure load. The shear stresses at the interface reached maximum concrete shear strength, which agrees well with the observed mode of failure where the failure took place at the interface between the deck panel and the haunch, as shown in Figs. 9–12. Fig. 17b shows the stress contours in z-direction (perpendicular to the loading direction) at the top of the haunch at failure load. The figure shows high stress concentration at the connector location where tension and compression stresses exceeded the concrete tensile and compressive strength, respectively. The stress distribution has abruptly changed at the connector location due to the horizontal load transfer between the shear connector and the concrete. It is worth

Table 4
Measured and predicted (FEA) load values at yielding and ultimate load levels.

Specimen ID	Shear pocket dimensions	Yielding load (kip)				Ultimate load (kip)			
		Measured	Average	FEA	Error	Measured	Average	FEA	Error
A1	HSS 7.5 × 0.188	104.4	126.4	101.4	23.9%	155.0	171.9	151.8	13.0%
A2	HSS 7.5 × 0.188	148.3				188.8			
B1	HSS 10 × 0.188	118.4	141.6	137.0	3.8%	152.8	164.7	187.0	14.6%
B2	HSS 10 × 0.188	164.7				176.5			
C1	HSS 10 × 0.25	125.0	123.5	137.0	10.8%	173.1	152.2	187.0	20.1%
C2	HSS 10 × 0.25	122.0				131.3			
D1	HSS 12.75 × 0.25	163.3	154.3	150.8	2.1%	163.2	154.3	150.8	2.1%
D2	HSS 12.75 × 0.25	145.3				145.3			
E1	HSS 14 × 0.25	196.3	207.8	184.3	12.0%	196.3	207.8	184.5	11.9%
E2	HSS 14 × 0.25	219.3				219.3			
				Average	10.5%			Average	12.3%

Note: 1 kip = 4.448 kN.

noting that the stress distribution in the transverse direction is similar to transverse stress dispersal distribution proposed by Johnson and Oehlers [17]. The development of these transverse stresses agrees well with the requirement of the European code [19] Section 6.2.4(4), which requires transverse reinforcement to be placed across the shear connection to prevent premature in-plane shear failure. Also, this confirms the need for haunch reinforcement described in the proposed design criteria to eliminate the propagation of these cracks, which could result in reducing the strength of the shear connection. Fig. 17c shows the stress distribution in the longitudinal direction (parallel to the loading direction) in the haunch. The plot shows high compression stresses in front of the shear connector with minor tension stresses behind the connector. The compression stresses are mainly due to bearing of the shear connector on the adjacent concrete. It was reported that concrete adjacent to the shear connector could experience high bearing stresses and can be as high as three times the concrete compressive strength.

Fig. 18a shows the geometry of the shear pocket connection. Hoop stress contours in the HSS at failure load is shown in Fig. 18b. The stress distribution indicates that half of the HSS is exposed to tension stresses (red contours) and the other half is exposed to compression stresses (blue contours). Fig. 18c shows the relationship between hoop stress (on y-axis) and the length along the circumference of the HSS (on x-axis), considering only half the circumference of the HSS. Stress distribution shown in Fig. 18b validates the concrete splitting hypothesis that is used in the proposed design criteria of the shear pocket connection where tension stresses are evidence in the high tri-axial compression zone (in front of the shear connector) and compression stresses behind the shear connector. This coincides with the concrete splitting behavior discussed in Johnson and Oehlers [17] based on experimental and analytical investigations.

5.3. Parametric study

In order to investigate the effect of the shear pocket's concrete compressive strength, and the shear pocket dimensions on the shear strength of the connection, nineteen FE models were developed. Fig. 14 shows the cross section and side view of modeled connection used for parametric studies. Twelve FE models were used to study the effect of concrete compressive strength of the shear pocket and seven FE models were used to study the effect of shear pocket dimensions. In order to study the effect of each parameter, the value of that parameter has been changed while other parameters were remained constant. The shear connectors considered, in all cases of study had a diameter of 38 mm (1.5 in.) and a total embedment length of 127 mm (5.0 in.) (L_e = 4.125 in.) with head diameter of 89 mm (3.5 in.) (d_h = 3.5 in.). In addition, the tensile yield and ultimate strength for the shear connector's material were 725 MPa (105 ksi) and 860 MPa (125 ksi), respectively. Haunch height was 89 mm (3.5 in.) in all specimens.

5.3.1. Effect of concrete compressive strength (f_c')

Effect of concrete compressive strength on the strength of shear pocket connections were studied using concrete compressive strength of 41 (6), 55 (8), 69 (10) and 83 (12) MPa (ksi). Other parameters such as yield and ultimate tensile strength of shear connector and shear connector diameter (d) were assumed to be constant. This parametric study was conducted on three shear pocket sizes: HSS 7.5 × 0.188, HSS 10 × 0.188, and HSS 14 × 0.25, to observe the general trend of the concrete compressive strength effect.

Fig. 19 shows the effect of concrete compressive strength on the interface shear strength. As the concrete compressive strength increases, the yield and the ultimate interface shear strength increases. Where the yield resistance level is defined as the end of linear resistance in the load-displacement relationship, when concrete fails at the haunch-pocket interface, while the ultimate resistance level is post yielding of the shear connectors. Based on the FEA results, the shear strength of the shear pocket connection increased to an average of 60% and 45% for yield and ultimate conditions, respectively, when the concrete compressive strength increased from 41 (6) to 83 (12) MPa (ksi). FEA results showed good correlation when it was compared to the experimental results.

5.3.2. Effect of shear pocket size

The effect of shear pocket dimensions on the interface shear strength of shear pocket connections was studied using seven different shear pocket sizes. The shear pockets ranged from HSS 7.5 × 0.188 to HSS 18 × 0.25. A concrete compressive strength of 55 MPa (8 ksi) was maintained throughout this study. Fig. 20 shows the yield and ultimate shear strength for a wide range of shear pocket sizes. FEA results were compared to the corresponding experimental test results discussed in previous section (when available). Both FEA and experimental results have shown significant increases in shear pocket connection strength as the pocket size increased in terms of the yield and the ultimate interface shear strength. For instance, based on FEA results, the yield and ultimate shear strength increased 35.5 and 23.2% when the shear pocket diameter increased from HSS 7.5 × 0.188 to HSS 10 × 0.25, respectively. The minimum and the maximum limits of a shear pocket with one-shear connector according the proposed design provisions, considering a connector diameter of 38 mm (1.5 in.), a head diameter of 89 mm (3.5 in.), effective embedment length of 100 mm (4 in.), and a construction tolerance of 100 mm (4 in.), are190 mm (7.5 in.) and 292 mm (11.5 in.), respectively. FEA results were comparable to experimental test results; where the shear pocket dimensions were within the proposed limits. However, when the shear pocket dimensions exceeded the maximum proposed limits (e.g., HSS 12.75 × 0.25 to HSS

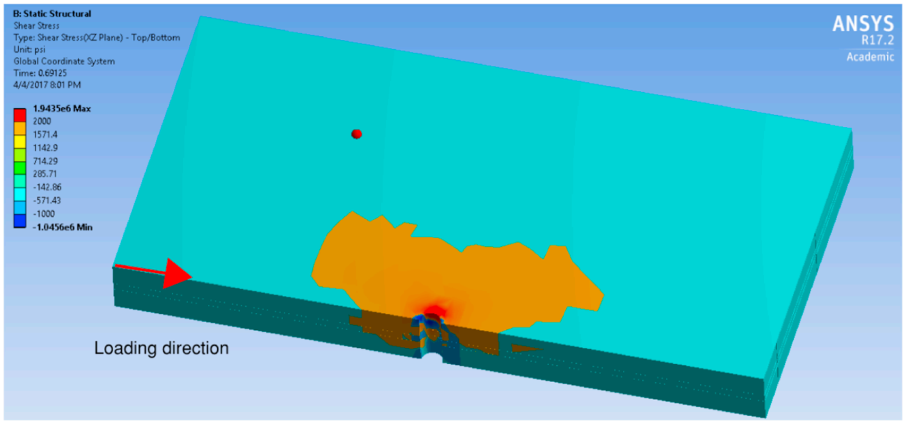

a) Shear stress contours

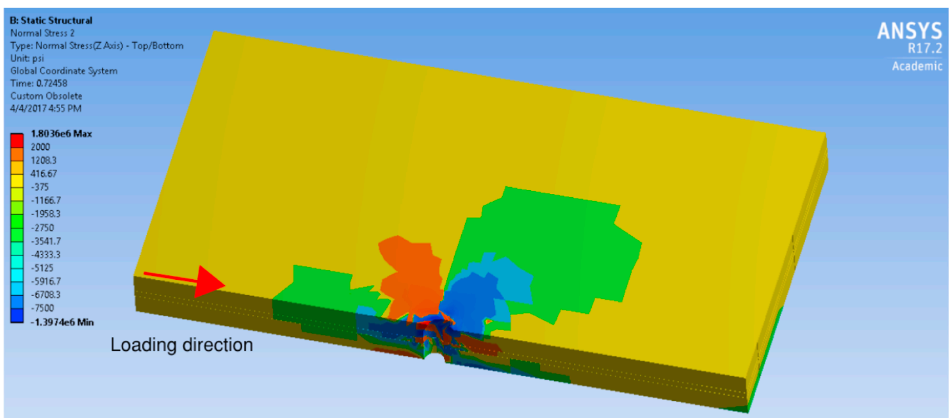

b) Stress contours in z-direction (perpendicular to the loading direction)

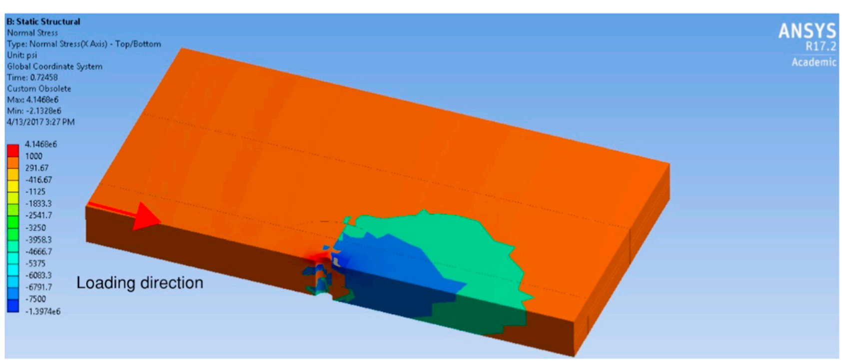

c) Stress contours in x-direction (parallel to the loading direction)

Fig. 17. Stress contours in the haunch (1 in. = 25.4 mm; 1 ksi = 6.9 MPa).

18 × 0.25), the concrete failed in a brittle mode (breakout failure); and the dowel action resistance was not achieved. This illustrates the need to have maximum dimensional limits for the shear pocket to prevent such a brittle failure and in order for the HSS to act effectively in resisting the concrete breakout failure.

6. Discussion

Sixteen push-off specimens were tested to evaluate the design procedures of shear pocket connections. Load-displacement relationships and modes of failure were examined for all the tested specimens where the proposed shear pocket dimension limits, HSS thickness, and the effect of haunch reinforcement were checked. All specimens had shear pocket dimensions that are within the proposed minimum and maximum limits except specimens “D” and “E” that had shear pocket with dimensions bigger than the proposed maximum limit. Testing results and modes of failure for these specimens showed satisfactory performance of the proposed shear pocket dimension limits. The mode of failure of the vast majority of specimens designed using dimensions within the proposed dimension limits were shearing off the threaded rod (connector) without any signs of concrete failure in the slab due to concrete splitting nor the haunch, as shown Fig. 9. However, once recommended upper shear pocket dimension limits were exceeded; concrete breakout failure took place inside the shear pocket, as shown in Fig. 10. Second, design thickness of the HSS was proven to provide adequate splitting resistance to the concrete deck, where no sign of longitudinal cracking was observed in the tested precast deck panels. The effect of transverse haunch reinforcement was proven to be critical

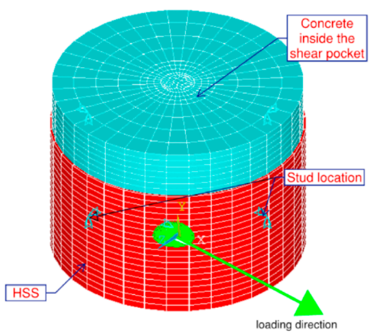

a) geometry of the shear pocket connection (deck panel is not shown for clarity)

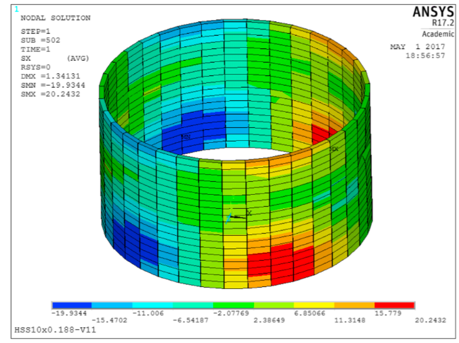

b) Hoop stress contours

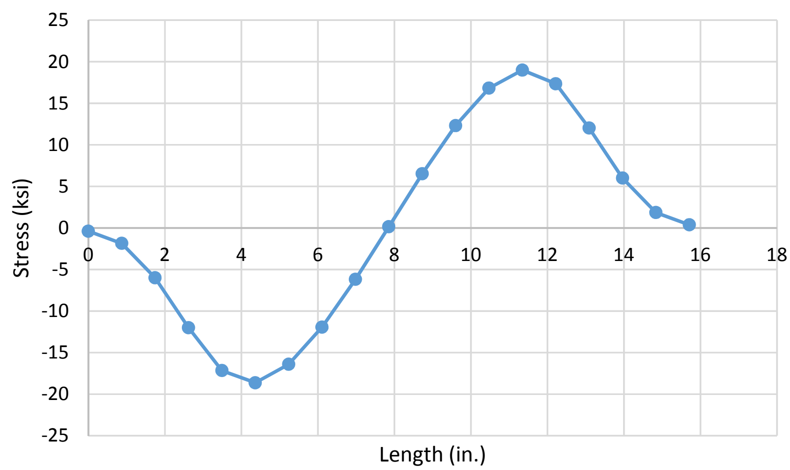

c) Hoop stress-length relationship (only half of the HSS is shown due to symmetry along xy-plane)

Fig. 18. Hoop stress distribution in the HSS (FEA) (1 in. = 25.4 mm; 1 ksi = 6.9 MPa).

to the interface shear strength according to push-off testing results by Hatami [16]. Therefore, in-plane shear provisions of EN 1992-1 [19] was adopted in this study to calculate the amount of required transverse reinforcement to prevent in-plane shear failure. It is worth noting that no sign of cracking was observed in the haunch of the tested specimens “A”, “B”, “C”, “D” and “E”. On the other hand, the haunch of specimens F and G experienced concrete failure in the haunch area due to a lack of transverse reinforcement, as shown in Figs. 11 and 12.

Specimens “F” and “G” were tested to verify the proposed design procedures/criteria for connections with multiple shear connectors. The shear pocket connections in these groups showed satisfactory interface shear strength and overall connection strength with respect to the proposed design procedures. However, these specimens experienced brittle concrete failure in the haunch area, which is attributed to the lack of transverse shear reinforcement. All tested push-off specimens exceeded the predicted interface shear strength by *fib* MC 2010 and AASHTO LRFD. The difference between the predicted and measured interface shear strength varied widely. For example, in specimens “A1” and “A2”, the measured interface shear strength was 230–268% of the predicted value using *fib* MC 2010 respectively, and 260–315% using AASHTO LRFD respectively. The predicted interface shear strength using both codes was controlled by the upper concrete strength limits. The main difference between test and code prediction values is attributed to the upper limit of shear strength values imposed by various code provisions as a function of the concrete compressive strength. These limits are conservative values adopted by the codes, which are based on experimental investigations found in the literature.

Nonlinear FEA was used to investigate the behavior of the tested push-off specimens. The main purpose of conducting these analyses was to better understand the behavior of the shear pocket connection in terms of stress distribution and load-displacement relationship. Load-displacement relationships from FE models of the push-off test correlated well with the experimental results for all cases. In addition, studying stress distribution in different elements helped understanding the behavior of the shear pocket connection and the adjacent concrete regions. Stresses observed in FE models conformed with the proposed design procedures/criteria of shear pocket connections. Parametric studies were also performed to investigate the effect of concrete compressive strength and shear pocket dimensions on the shear pocket connection strength. It is concluded that both parameters have crucial effects on the shear pocket connection strength. Increasing the concrete compressive strength from 42 MPa (6 ksi) to 84 MPa (12 ksi) resulted in increasing the connection strength to a range of 42–72% for various shear pocket sizes. In addition, increasing the shear pocket dimensions increases the shear pocket strength as long as the selected shear pocket dimensions are within the proposed dimension limits. However, exceeding the maximum limits of the proposed criteria would result in brittle failure for concrete inside the shear pocket without achieving the dowel action resistance.

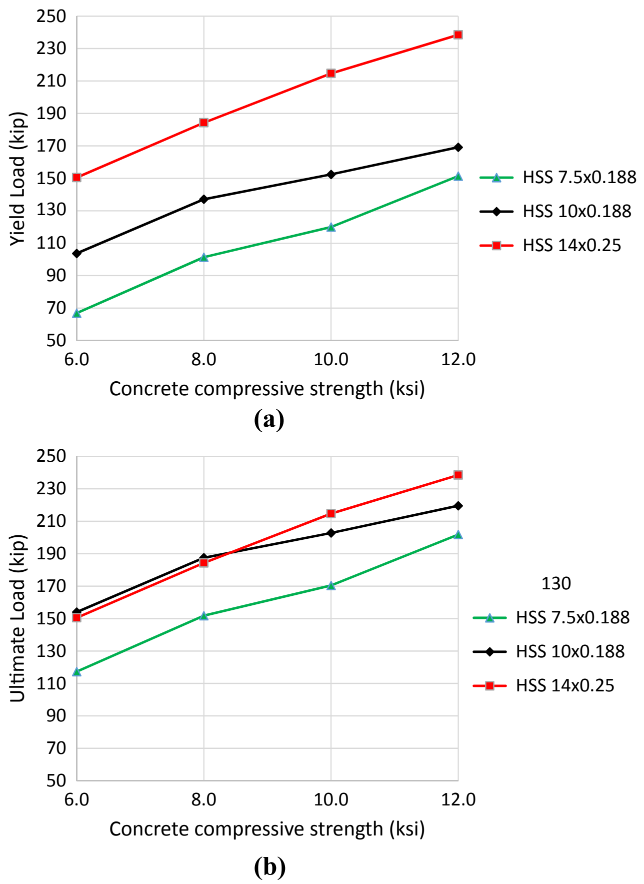

Fig. 19. Concrete compressive strength effect on: a) yield shear strength and b) ultimate shear strength using FEA (1 kip = 4.448 kN; 1 ksi = 6.9 MPa).

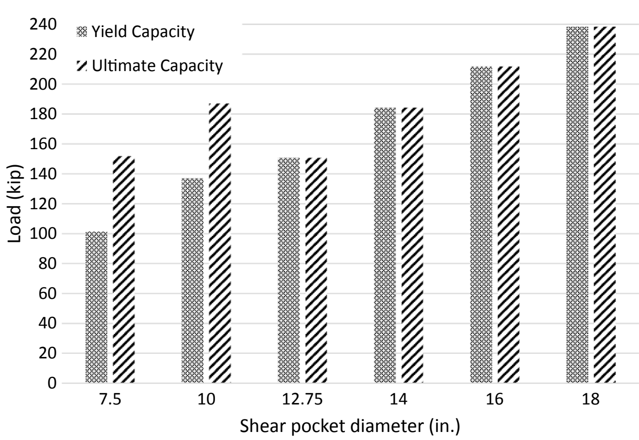

Fig 20. Effect of shear pocket size on interface shear resistance using FEA (1 in. = 25.4 mm; 1 kip = 4.448 kN).

7. Conclusions

In this paper, design criteria for HSS formed shear pocket connections used in full-depth precast concrete deck systems were developed to address the following failure mechanisms:

1. concrete splitting, which determine the required deck transverse reinforcement and HSS thickness;
2. in-plane shear, which determine the required haunch transverse reinforcement to avoid concrete crushing;
3. concrete breakout, which determine the maximum pocket dimensions to prevent concrete breakout; and
4. HSS pullout, which determine the number of studs required to provide adequate anchorage between the HSS and deck panel.

The experimental investigation conducted to validate the proposed design criteria consisted of 16 push-off specimens that include rectangular and circular HSS formed shear pockets in concrete and steel girders. Testing results had shown that HSS-formed shear pocket connections performed best when all the proposed design procedures/criteria are satisfied. The mode of failure of those specimens was shearing off the connectors after reaching their ultimate capacity. Other specimens experienced premature concrete failure when the shear pocket dimensions exceeded the recommended upper limits and/or when transverse reinforcement was not provided.

A parametric study was conducted using Finite Element Analysis (FEA) to investigate the effect of concrete compressive strength and shear pocket dimensions on the connection capacity. It is concluded that both parameters have a vital effect on the shear pocket connection strength. As the concrete compressive strength increases from 42 MPa (6 ksi) to 84 MPa (12 ksi), the shear strength of the connection increases 42–72% depending on the pocket sizes. In addition, increasing the shear pocket dimensions increases the connection strength as long as it is within the proposed dimension limits. For example, using 18 in. diameter circular pockets results in a 57% increase in the shear strength of the connection compared to using 7.5 in. diameter circular pocket.

Appendix A. Supplementary material

Supplementary data to this article can be found online at https://doi.org/10.1016/j.engstruct.2018.11.003.

References

[1] Accelerated bridge construction manual - experience in design, fabrication and erection of prefabricated bridge elements and systems. Report FHWA-HIF-12-013, McLean, VA: Office of Bridge Technology, Federal Highway Administration (FHWA); 2011.
[2] American Association of State Highway and Transportation Officials (AASHTO). LRFD Bridge Design Specifications. 7th ed. Washington, DC; 2014.
[3] Tawadrous R, Morcous G. Interface shear resistance of clustered shear connectors for precast concrete bridge deck systems. Eng Struct 2018;160:195–211. https://doi.org/10.1016/j.engstruct.2018.01.007. ISSN 0141-0296.
[4] Carter III JW, Hubbard FK, Oliva MG, Pilgrim T, Poehnelt T. Wisconsin's use of full-depth precast concrete deck panels keeps interstate 90 open to traffic. Prestressed/Precast Concr Inst (PCI) J 2007;52(1):2–16.
[5] Scholz DP, Wallenfelsz JA, Lijeron C, Roberts-Wollmann CL. Recommendations for the connection between full-depth precast bridge deck panel systems and precast I beams. Final report no. FHWA/VTRC 07-CR17. Virginia Transportation Research Council, June; 2007. p. 78.
[6] Badie SS, Tadros MK. Full-depth, precast-concrete bridge deck panel systems. Washington, D.C.: Transportation Research Board; 2008. National Cooperative Highway Research Program, NCHRP 12–65, Report 584.
[7] Sullivan SR, Wollman CLR, Swenty MK. Composite behavior of precast concrete bridge deck-panel systems. PCI J 2011;56(3):43–59.
[8] Davies C. Tests on half-scale steel concrete composite beams with welded stud connectors. Struct J Eng 1969;47(1):29–40.
[9] Chapman JC. Composite construction in steel and concrete: the behavior of composite beams. Struct Eng 1964;4:115–25.
[10] Toprac AA, Dale GE. Composite beams with a hybrid tee steel section. J Struct Eng ASCE 1967;93(5):309–22.
[11] Taylor HPJ. Investigation of the forces carried across cracks in reinforced concrete beams in shear by interlock of aggregate (No. TR 42.447 Tech. Rpt.); 1970.
[12] Kulliman RB, Hosain MU. Shear capacity of stub-girders: Füll scale tests. ASCE J Struct Eng 1985;III(1):56–75.
[13] Oehlers DJ. Splitting induced by shear connectors in composite beams. J Struct Eng ASCE 1989;115(2):341–62.
[14] Oehlers DJ, Johnson RP. The strength of stud shear connectors in composite beams. Struct Eng 1987;65(2):44–8. London, England.
[15] Oehlers DJ. Stud shear connector for composite beams PhD thesis University of Warwick; 1980.
[16] Hatami A. Design of shear connectors for precast concrete decks in concrete girder bridges Doctorate Dissertation University of Nebraska-Lincoln; 2014.
[17] Johnson RP, Oehlers DJ. Analysis and design for longitudinal shear in composite T-beams. Proceedings of the institution of civil engineers, London, England, Part 2,

vol. 71, December; 1981. p. 989–1021.
[18] Flamant A. Sur la répartition des pressionsdansunsoliderectangulaire chargé transvers alement. Compte Rendu Acad Sci Paris 1892;114:1465. [in German].
[19] Eurocode 2 (EC 2). Design of concrete structures – Part 1-1: general rules and rules for buildings. CEN, EN 1992-1-1, Brussels; 2004.
[20] Mattock AH, Hawkins NM. Shear transfer in reinforced concrete recent research. PCI J 1972;17(2):55–75.
[21] Eurocode 4 (EC 4). Design of composite steel and concrete structures – Part 2: general rules and rules for bridges. CEN, EN 1994-2, Brussels; 2005.
[22] Teraszkiewicz JS. Test on stud shear connectors. Road Laboratory Technical Note No. 36, Crowthorne, U.K., December; 1965.
[23] British Standard (BS) 5400. Steel, concrete and composite bridges: Part 5: code of practice for design of composite bridges. London: British Standards Institution; 1979.
[24] Oehlers DJ, Bradford MA. Composite steel and concrete structural members: fundamental behavior. 1st ed Oxford: Pergamon Press; 1995. 588 p. ISBN 0080419194.
[25] American Concrete Institute (ACI) Committee 318. Building code requirements for structural concrete and commentary (ACI 318 R-14), Farmington Hills, MI; 2014.
[26] CSA. Canadian Highway Bridge Design Code. CAN/CSA-S6-00. Rexdale (Ontario, Canada): Canadian Standards Association; 2000.
[27] AISC. Steel construction manual. 14th ed. Chicago (IL): American Institute of Steel Construction; 2010.
[28] Shahrooz BM, Miller RA, Harries KA, Russell HG. Design of concrete structures using high-strength steel reinforcement. NCHRP Report 679. Washington, D.C.: Transportation Research Board; 2011.
[29] Randl Norbert. Design recommendations for interface shear transfer in fib Model Code 2010. Struct Concr J FIB 2013;14(3):230–41.
[30] Mishima T, Suzuki A, Maekawa K. Nonelastic behavior of axial reinforcement subjected to axial and slip deformation at the crack surface. J Am Concr Inst ACI 1995;92(3):380–5.
[31] Kono S, Tanaka H, Watanabe F. Interface shear transfer for high strength concrete and high strength shear friction reinforcement. In: The fourth U.S.-Japan workshop on performance-based earthquake engineering methodology for reinforced concrete building structures, Toba, Japan; 2002.
[32] Randl N. Untersuchungen zur Kraftübertragung zwischen Altund Neubeton bei unterschiedlichen Fugenrauhigkeiten. (Investigations into the force transfer between old and new concrete with various joint roughnesses); Dissertation, Universität Innsbruck, 379 S; 1997 [in German].
[33] Federation International du Béton (fib). Model Code 2010, final draft. Fib Bulletin Nos. 65/66, Lausanne; 2012.
[34] Cannon R, Godfrey D, Moreadith F. Guide to the design of anchor bolts and other steel embedment. Concr Int 1981(July):28–41.
[35] Lee N, Kim K, Bang C, Park K. Tensile-headed anchors with large diameter and deep embedment in concrete. ACI Struct J 2007;104(4):479–86.
[36] CEB. Fastenings to concrete and masonry structures: state of the art report. London: Thomas Telford Service Ltd.; 1997.
[37] Tawadrous R. Design of shear pocket connections in full-depth precast concrete bridge deck systems Doctorate Dissertation University of Nebraska-Lincoln; 2017.
[38] Mattock AH. Shear friction and high-strength concrete. ACI Struct J 2001;98(1):50–9.
[39] Wallenfelsz JA. Horizontal shear transfer for full-depth precast bridge deck panels Master's Thesis Blacksburg (VA): Polytechnic Institute and State University; 2006.
[40] ANSYS help. Release 17.2 Documentation for ANSYS; 2016.
[41] Badiger S, Malipatil M. Parametric study on reinforced concrete beam using ANSYS. Civ Environ Res 2014;6(8). ISSN 2224-5790.